

Princetonlaan 6
3584 CB Utrecht
P.O. Box 80015
3508 TA Utrecht
The Netherlands

www.tno.nl

T +31 88 866 42 56
F +31 88 866 44 75

TNO report**TNO 2015 R11367****Response of induced seismicity to production
changes in the Groningen field**

Date	10 November 2015
Author(s)	Karin van Thienen-Visser, Danijela Sijacic, Manuel Nepveu, Jan-Diederik van Wees, Jenny Hettelaar
Copy no	
No. of copies	
Number of pages	56 (incl. appendices)
Number of appendices	3
Sponsor	
Project name	F2 - Groningen ondergrond
Project number	060.14108/01.07.03

All rights reserved.

No part of this publication may be reproduced and/or published by print, photoprint, microfilm or any other means without the previous written consent of TNO.

In case this report was drafted on instructions, the rights and obligations of contracting parties are subject to either the General Terms and Conditions for commissions to TNO, or the relevant agreement concluded between the contracting parties. Submitting the report for inspection to parties who have a direct interest is permitted.

© 2015 TNO

Summary

Before the next update of the Groningen production plan in 2016, the Minister of Economic Affairs reconsiders his decision concerning production measures in the Groningen gas field in relation to safety every half year. Next update is due in December 2015. In July 2015 State Supervision of Mines requested TNO to give an update on the seismicity of the Groningen field and to assess the response of induced seismicity to production changes in the Groningen field.

This evaluation has been performed within the framework of the yearly program for the Ministry of Economic Affairs (reference AGE 15-10.018).

Approach

So far, reservoir compaction is used as a proxy for the occurrence of seismic events in Groningen (cf. NAM 2013, TNO 2013). However, fault behavior is more important than compaction for understanding seismicity in Groningen (Figure A; TNO, 2015).

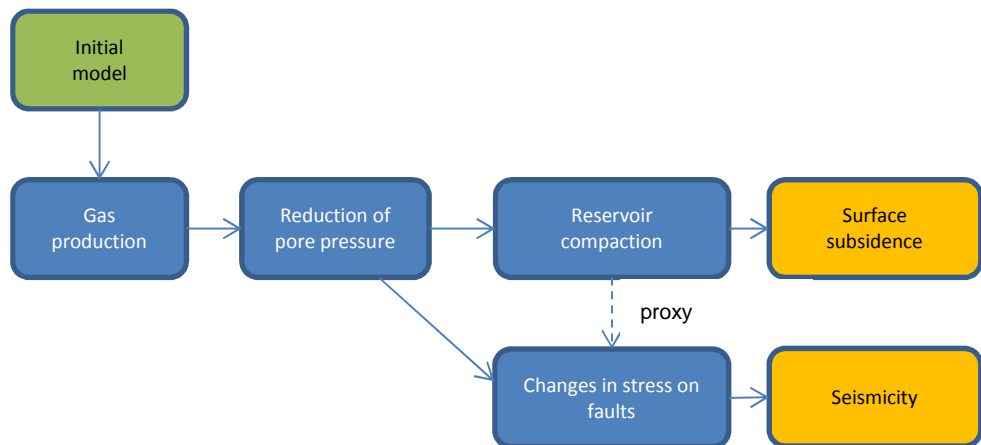


Figure A. Schematic of the relation between gas production and seismicity.

Response of induced seismicity to production changes in the Groningen field

The relation between production, faults and seismic events is studied using a three-step approach. The first step is visual inspection of the observations. As a second step statistical studies have been performed on the seismicity. In addition correlations between measured production and observed seismicity have been analysed. Statistics cannot prove causal relations. Hence, the third and last step is to check whether the statistical correlations are physically meaningful by applying a geomechanical model.

Visual inspection

In the period from 1996 to 2002/2003, the production changes (3 maxima's) are not followed by seismicity changes (1 maximum). Since 2002/2003 production changes are followed by seismicity changes with a delay of 4-8 months. Following the production reduction in January 2014, event densities show a decrease in the center of the field. Overall, event densities have decreased in 2014 and 2015 compared to earlier years.

Statistical analysis

The results show a statistically significant relation between production and seismicity within the framework of Bayesian analysis:

- a constant event rate up to ~2003,
- an increasing event rate from 2003 to 2014,
- in the center of the field a lower event rate from early 2014 to now,
- in the southwest of the field a higher event rate from early 2014 to now,
- seasonality in the number of seismic events, and a delay of 2 to 8 months between production changes and seismicity.

Fault model

Geomechanical analysis provides a physical, fault based mechanism between (changes in) production and seismicity. Modelling of a single fault in a synthetic reservoir demonstrates characteristics of the observed seismicity in the Groningen field.

Main finding

The effect of existing production measures (in particular those of January 2014) on seismic events has resulted in a decreased rate of seismic events in the center of the field in the period 2014 to September 2015. Please note that earlier work (letter AGE 14-10.016, accompanying report TNO, 2013) suggests that such an effect is temporary and also depends on the future production scenario (i.e. a lower production rate may extend the effect in time).

Update on the seismicity of the Groningen field September 2015

Due to the installation of additional borehole seismometers the number of observed, smaller events ($M_L < 1.0$) has increased considerably in 2015.

A limited number of $M_L > 2.0$ events have occurred, the largest of which was the event near Hellum ($M_L = 3.1$) on September 30th 2015.

In Groningen seismic events first occurred in the center of the field. Over time and with continuing production, $M_L > 1.5$ events are gradually spreading out from the center (NAM, 2013). The Hellum event occurred south of previous $M_L > 3.0$ events and fits in this trend.

Based on assumptions for a Groningen production profile from January 2014 to January 2017, TNO (2014a) prognosed compaction (as a proxy for potential seismic moment). Near the location of the Hellum event the assumed production profile is close to the actual production profile, especially in the year 2014. Prognosed potential seismic moment at this location is about 1.6 times higher in January 2017 compared to January 2014 (Figure B).

Please note that a single event (such as the Hellum event) cannot demonstrate the validity or quality of any prognosis. Note also that the validity of the 2014 prognosis of potential seismic moment (Figure B) depends on whether the actual production is similar to the assumed production scenario of TNO (2014a).

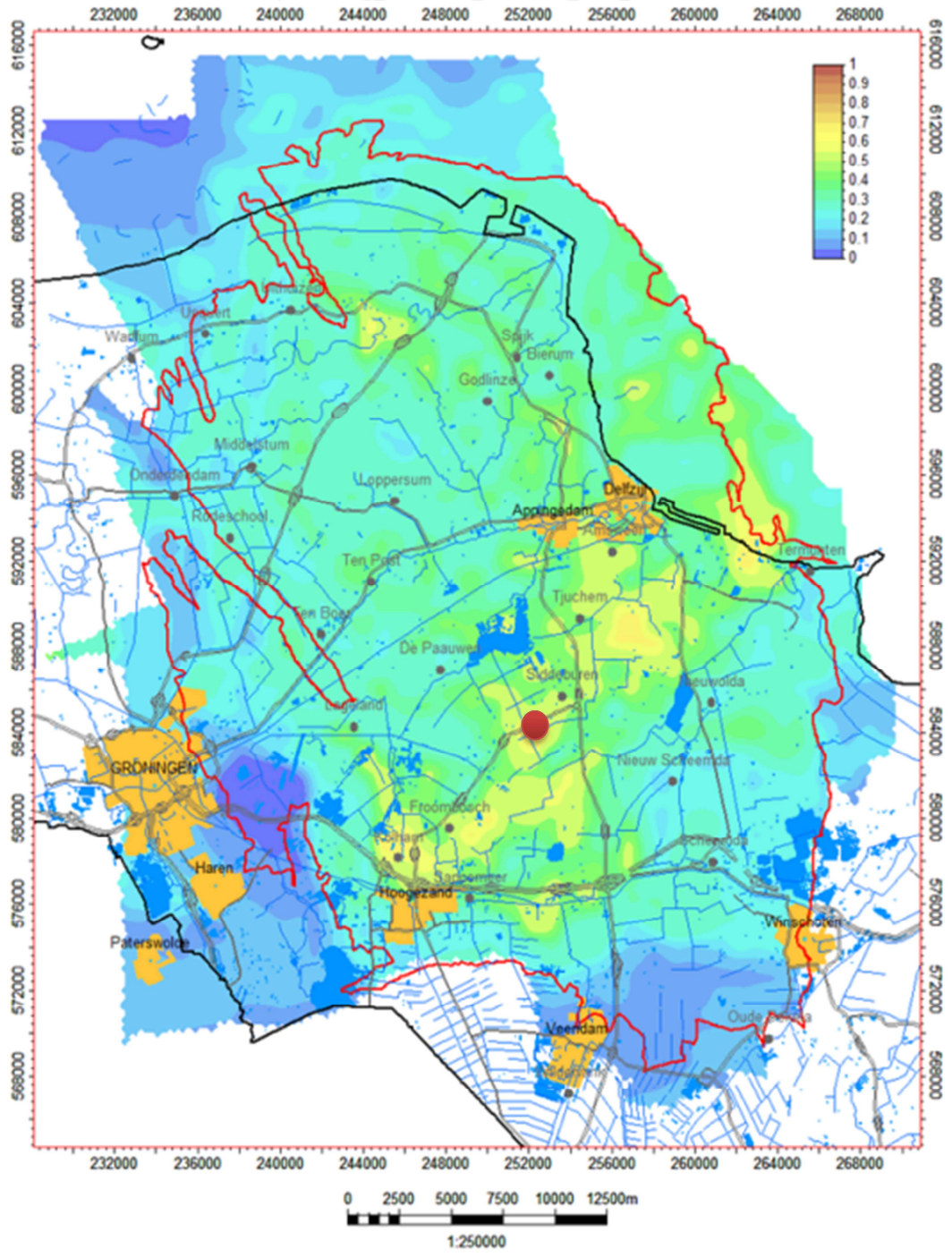


Figure B. Increase in potential seismic moment (per unit compaction) from 2014-2017, source TNO (2014a). The location of the Hellum event is indicated in red.

Contents

	Summary	2
1	Introduction.....	9
2	Observations of production and induced seismicity in Groningen	11
2.1	Production.....	11
2.2	Observations of seismic events in 2015.....	12
2.3	Event density maps	18
2.4	Visualization of events and production	19
3	What do we know about the relation between production and seismicity?....	24
3.1	Bayesian change point model	25
3.2	Bayesian Model comparison	28
3.3	Seasonality	31
4	The causal relation between production and seismicity.....	34
4.1	Numerical model for rupture of a single fault.....	34
5	Findings.....	39
6	References	40
7	Signature	43
	Appendices	
	A Normalization of cross-correlations	
	B Event density maps	
	C Production density maps	

Figures

Figure 1-1. Schematic description of the relation between gas production and seismicity.	9
Figure 2-1. Production of the southwest clusters (Froombosch (FRB), Slochteren (SLO) and Kooipolder (KPD)) as well as the clusters Tjuchem (TJM), Siddeburen (SDB) and Oudeweg (ODW) for the period January – Augustus in 2014 (top) compared to 2015 (bottom).....	11
Figure 2-2. Top: Density of Production (number of Nm ³ per km ²) from July 2012 to July 2015. The producing/non-producing clusters are indicated by the colored small circles. Bottom: Difference in production (in Nm ³) between the indicated periods. A negative (green) difference indicates a lower production in the later period compared to the earlier period. Larger size figures are in appendix C. .	12
Figure 2-3. Observed seismic events with magnitude above $M_L=1.0$ from January to October 2015. The color scale indicates the magnitude of the events and the Groningen contour is indicated in red.....	13
Figure 2-4. Number of events in 2013, 2014 and 2015 (up to 5 th October) in magnitude bins.	14
Figure 2-5. Location of the event near Hellum (red) with respect to the producing clusters (green) and the faults of the static geological model (dark red lines). .	15
Figure 2-6. Increase in compaction and increase in potential seismic moment in 2014-2017 (The value 1.0 indicating a doubling of potential seismic moment which could be released), taken from TNO (2014a, Figures 6-2 and 6-4). The location of the Hellum event is indicated in red.	16
Figure 2-7. Production of clusters (FRB, KPD, SDB, SLO, TJM, ODW) yearly from 2012 to 2014 (a) and monthly in 2015 (b).	17
Figure 2-8. Top: Event density (number of events per km ²) from July 2012 to July 2015. The observed events and their magnitudes are indicated by the colored small circles. Bottom: Difference in event density between the indicated periods. A negative (green) difference indicates a lower event density in the later period compared to the earlier period. Larger size figures are in appendix B.....	18
Figure 2-9. Moving sum of the yearly seismicity with magnitudes larger than specified magnitude; number of events indicated at i.e. January 2015, is the total number of events between 1 st January 2014 and 1 st January 2015. The difference between the figures is the magnitudes and the range of the number of events.	19
Figure 2-10. Moving sum of yearly production and yearly seismicity (all events from $M_L>1.0$) using a delay between production and seismicity of 4 (a), 6 (b) and 8 (c) months.....	20
Figure 2-11. Moving sum of yearly production and yearly seismicity (all events from $M_L>1.5$) using a delay between production and seismicity of 4 (a), 6 (b) and 8 (c) months.....	21
Figure 2-12. Moving sum of half-yearly production and half-yearly seismicity (all events from $M_L\geq 1.0$) using a delay between production and seismicity of 4 (a), 6 (b) and 8 (c) months.	22

Figure 2-13. Moving sum of half-yearly production and half-yearly seismicity (all events from $M_L \geq 1.5$) using a delay between production and seismicity of 4 (a), 6 (b) and 8 (c) months.	23
Figure 3-1 Number of events occurring within the contour of the Groningen gas field as a function of time from 1996 and Magnitude (M_L) for the whole catalogue (a) and the declustered catalogue (b).	25
Figure 3-2. Illustration of the Bayesian change point model in the case of a single step increase (a) or an increasing rate with time (b).	26
Figure 3-3. The pre and post date change event rates for time intervals T_0 and T_1 (a) and T_2 to T_4	26
Figure 3-4 Illustration of the relation between the Bayesian point change analysis and the number of events per year from the Groningen seismicity catalog (from Figure 2-9). Change points for time intervals T_1 and T_4 and corresponding pre and post event rates are shown.	27
Figure 3-5a. The pre change date event rate (in events/day) – dashed line and the post change date event rates (in events/day) for the change point on May 19 th 2014 and b. The probability of change in time over the period of 2012 up to now (Sept. 2015).	28
Figure 3-6. Correlation per year for all magnitudes above $M_L=1.0$	32
Figure 3-7. The stacked correlation in 2012 between production on a monthly basis and the number of seismic events for all magnitudes of the seismic catalogue (source: KNMI), for magnitudes larger than $M_L \geq 1.0$ and for $M_L > 1.5$ (a) and same for the declustered catalogue (b).	33
Figure 3-8. Tests of significance of correlation: test with a constant seismicity over the year (a) and test with a perfect sinusoidal behavior of the seismicity (b).	33
Figure 4-1 Model geometry (from Van Wees et al., 2014).	35
Figure 4-2 From left to right, displacement [m], Coulomb stress below failure criterion (red means fault should slip) and modelled seismic events (magnitude versus time on top and seismic moment versus time on the bottom), for in-situ horizontal to vertical effective stress ratio of 0.34. From top to bottom: initial situation, after 2000, 4000 steps and 5000 time steps. The in-situ stress on the fault is critical causing events after 10% of the reservoir depletion.	36
Figure 4-3 From left to right, displacement [m], Coulomb stress below failure criterion [bar] (red means fault should slip) and modelled seismic events (magnitude versus time on top and seismic moment versus time on the bottom) for in-situ horizontal to vertical effective stress ratio of 0.43. From top to bottom: initial situation, after 2000, 4000 steps and 5000 time steps. The in-situ stress on the fault is sub- critical causing events after 30% of the reservoir depletion.	37

Tables

Table 2-1. Induced seismicity (source: KNMI) of the Groningen field. Events larger than $M_L=2$ in 2015.....	14
Table 3-1. Overview of investigated time intervals and the resulting change points in event rate. The Bayes factor determines the odds of change point model above one single constant rate model.....	26
Table 3-2. Bayes factors and number of events for the model comparison between a stationary event rate and an increasing event rate. Data since 17 th January 2014.....	29
Table 3-3. Bayes factors and number of events for the model comparison between a stationary event rate and an increasing event rate. Data since 17 th January 2014.....	29
Table 3-4. The number of events with magnitude $M_L \geq 1.0$ in the regions Central (C), Southwest (SW) and Other (O) as a function of the number of days since the start of observed seismicity on December 5 th 1991.	31
Table 3-5. The event rate, including standard deviation, in the regions Central (C), Southwest (SW) and Other (O) as a function of the number of days since the start of seismicity on December 5 th 1991.	31

1 Introduction

Background

Since 2012, when the largest induced event observed so far occurred in the Groningen gas field, the seismicity induced by gas depletion has been under investigation. Production reached a high of 54 bcm in 2013, and was subsequently lowered by the Minister of Economic Affairs to 42,5 bcm in 2014 and 30 bcm in 2015 (EZ 2014, EZ 2015a,b). Additionally, production from the five central clusters in the field has been limited to 3 bcm per year since January 17th 2014.

Scope

Since the beginning of 2015, the minister revises his decision on the caps of the gas production in Groningen every half year. The next update is expected in December 2015.

In support of their advice for this update, State Supervision of Mines (SSM) has requested the following technical evaluations from TNO-AGE:

- Effect of the production reduction on seismicity
- Update on the seismicity of the Groningen field

These evaluations are performed within the framework of the yearly work plan for the Ministry of Economic Affairs (reference AGE 15-10.018).

Report Setup

Reduction of pressure in the reservoir causes both compaction as well as changes in stress on faults in the reservoir (Figure 1-1). Reservoir compaction leads to subsidence, which is visible at the surface. Changes in stress on faults lead to seismic events. It is technically more feasible to compute compaction which is why reservoir compaction has been used as a proxy for the occurrence of seismic events in Groningen (NAM 2013, TNO 2013). As indicated in TNO (2015) the presence of faults is more important for the seismicity than compaction. This was substantiated by the difference between the pattern of seismicity and the compaction pattern over the field. Therefore in this report we focus on the relation between the existing faults and the seismic events.

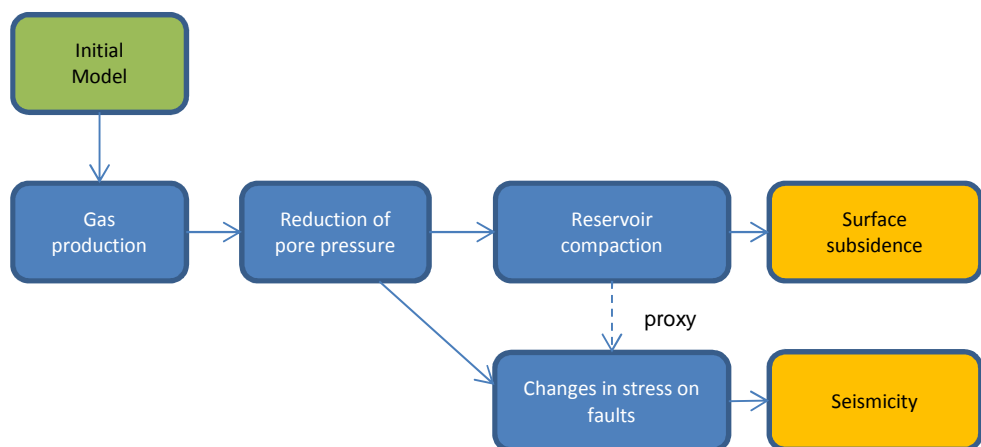


Figure 1-1. Schematic description of the relation between gas production and seismicity.

Chapter 2 reports the observations (events and production) both in the past as well as the latest observations in 2015. In Chapter 3 we review what we know about the relation between production changes and the occurrence of seismicity using statistical methods. The statistics in the period since January 2014 (period of production reductions) are analysed. As statistics cannot prove a causal relation between production and seismicity, Chapter 4 describes the physical relation between production and seismicity using a geomechanical model of a single fault. The results are summarized in Chapter 5.

2 Observations of production and induced seismicity in Groningen

In this chapter first the production in 2015 is shown (section 2.1). Secondly, the seismicity of the Groningen field is evaluated using recent observations (section 2.2), event densities (2.3), and the visual relation between (half)-yearly production and seismicity (2.5).

2.1 Production

The current status of the regional limits on gas production are:

- 3 bcm per year for the Loppersum clusters (Leermens (LRM), Overschild (OVS), De Paauwen (PAU), Ten Post (POS) and 't Zand (ZND))
- 2.0 bcm per year for the Eemskanaal (EKL) cluster
- 9.9 bcm per year for the Southwest clusters (Froombosch (FRB), Kooipolder (KPD), Slochteren (SLO), Zuiderveen (ZDV), Spitsbergen (SPI), Tusschenklappen (TUS), Sappemeer (SAP))
- 24.5 bcm/year for the East clusters (all other clusters)

Additionally total gas production has been limited to 16.5 bcm for January 2015 to July 2015 and 30 bcm for the whole of 2015.

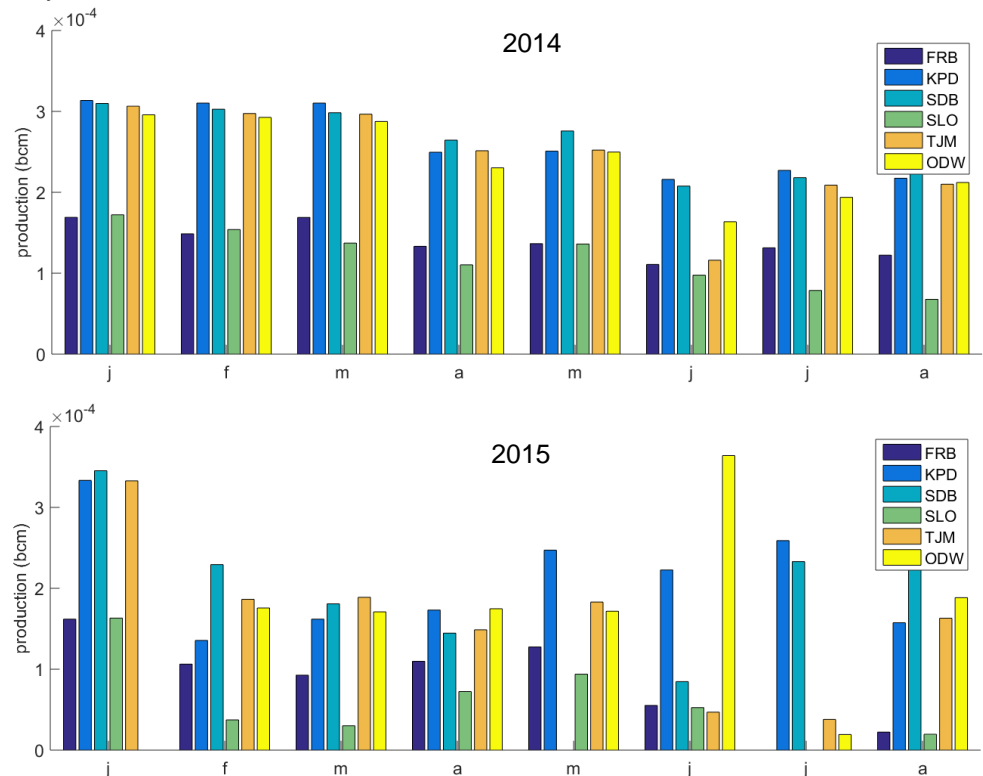


Figure 2-1. Production of the southwest clusters (Froombosch (FRB), Slochteren (SLO) and Kooipolder (KPD)) as well as the clusters Tjuchem (TJM), Siddeburen (SDB) and Oudeweg (ODW) for the period January – August in 2014 (top) compared to 2015 (bottom).

Production for the southwest clusters (FRB, KPD, SLO) has been reduced in 2015 (Figure 2-1) compared to the previous years. Up to the end of August 2015, the clusters FRB, KPD and SLO have produced $3.5 \cdot 10^{-3}$ bcm, which is lower compared to the $4.8 \cdot 10^{-3}$ bcm of January to the end of August 2014. Production has also been lowered in the east of the field (for example the clusters TJM, SDB, ODW in Figure 2-1). Additionally, production in 2015 has been more erratic compared to 2014 (Figure 2-1).

2.1.1 Production density maps

Figure 2-2 shows the production density for the period July 2012 to July 2015. The densities were determined using a Kernel Density (standard GIS application) with a radius of 5 km and a cell size of 50 m. Since January 2014 production is reduced in the center of the Groningen field. In 2014, production was increased in the south and southeast of the field to compensate the reduction in the center of the field. In January 2015, production in the southwest of the field was limited as well, leading to decreases in production in 2015. This is however not visible in these density maps as they are from July 2014 to July 2015. Production in the second half of 2014 was such that the total production still shows an increase in the southwest area and the area around Tjuchem even though production has decreased since January 2015.

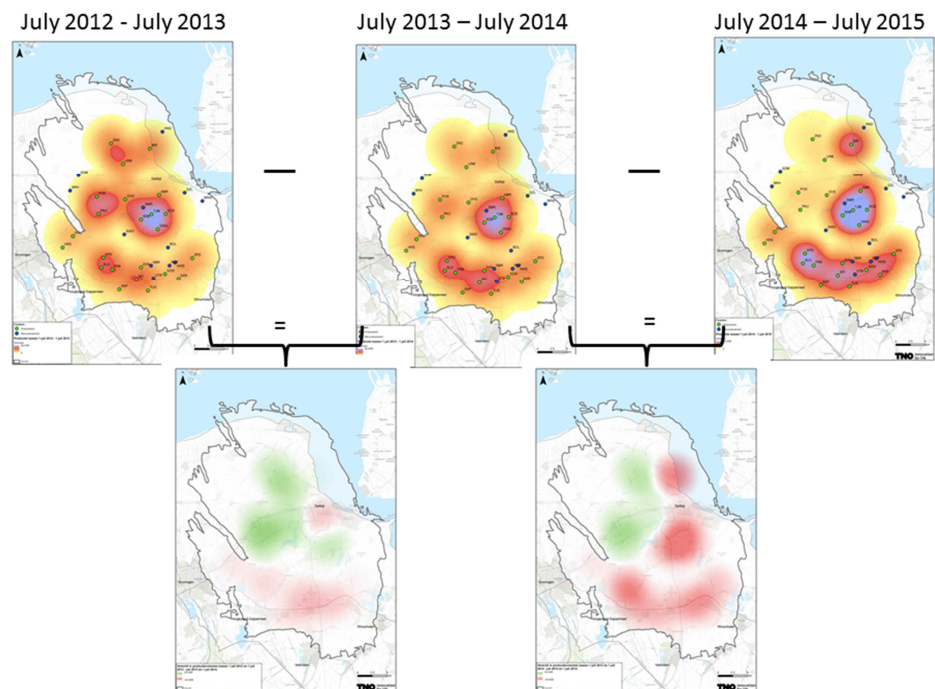


Figure 2-2. Top: Density of Production (number of Nm³ per km²) from July 2012 to July 2015. The producing/non-producing clusters are indicated by the colored small circles. Bottom: Difference in production (in Nm³) between the indicated periods. A negative (green) difference indicates a lower production in the later period compared to the earlier period. Larger size figures are in appendix C.

2.2 Observations of seismic events in 2015

Figure 2-3 shows the observed seismic events with a magnitude above $M_L=1.0$ from January to September 2015. The largest event in this period was observed in Hellum (30-09-2015) with a magnitude of $M_L=3.1$.

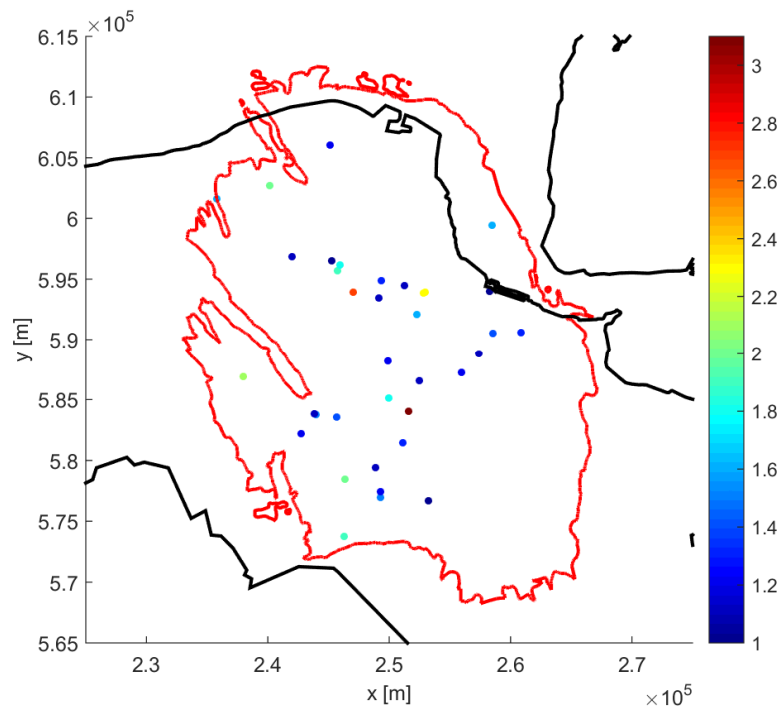


Figure 2-3. Observed seismic events with magnitude above $M_L=1.0$ from January to October 2015. The color scale indicates the magnitude of the events and the Groningen contour is indicated in red.

2.2.1 *More observations of small events*

In 2014, new borehole seismometers have been installed in the Groningen area (<http://www.knmi.nl/nederland-nu/seismologie/stations>). Since this installation the catalogue of the KNMI shows an increase in the number of smaller events ($M_L < 1.0$) that have been localized (Figure 2-4) in 2015. Previously, without the new network, those events would mostly not have been localized and included into the seismic catalogue. The magnitude for which the catalogue is complete over the Groningen field before the new network is somewhere between magnitudes $M_L=1.0 - 1.5$ (KNMI 2012, Pijpers 2015). This magnitude of completion has probably decreased after the installation of the new borehole seismometers.

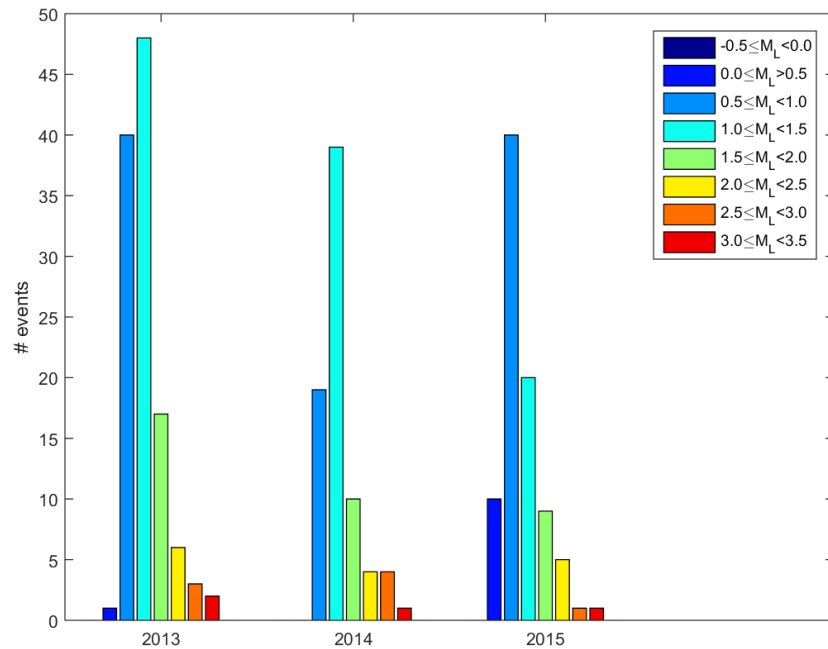


Figure 2-4. Number of events in 2013, 2014 and 2015 (up to 5th October) in magnitude bins.

2.2.2 Events above $M_L=2.0$

Table 2-1 shows the induced seismicity of the Groningen field in 2015 for all events larger than $M_L=2.0$.

Table 2-1. Induced seismicity (source: KNMI) of the Groningen field. Events larger than $M_L=2$ in 2015.

Event	date	M_L
Wirdum	06-01-2015	2.7
Appingedam	25-02-2015	2.3
Appingedam	24-03-2015	2.3
Thesinge	07-07-2015	2.1
Hellum	30-09-2015	3.1

In our previous report (TNO, 2015) we already discussed the events near Appingedam and Wirdum. We concluded that the increase of events near Appingedam may indicate that the pressure wave associated with the continuing production in the nearby producing clusters of Amsweer (AMR), Siddeburen (SDB) and Tjuchem (TJM) causes compaction which may explain the increased seismic activity in this area. For the Wirdum event we suggested this might be caused by a sudden increase in production in the nearest Ten Post (POS) cluster in December 2014. For both phenomena we concluded that it is too early to draw firm conclusions and more observations are needed to support our explanations. The event in Thesinge is close to the Eemskanaal (EKL) cluster which has been reduced in production since January 2015 to a maximum of 2 bcm per year (EZ 2015).

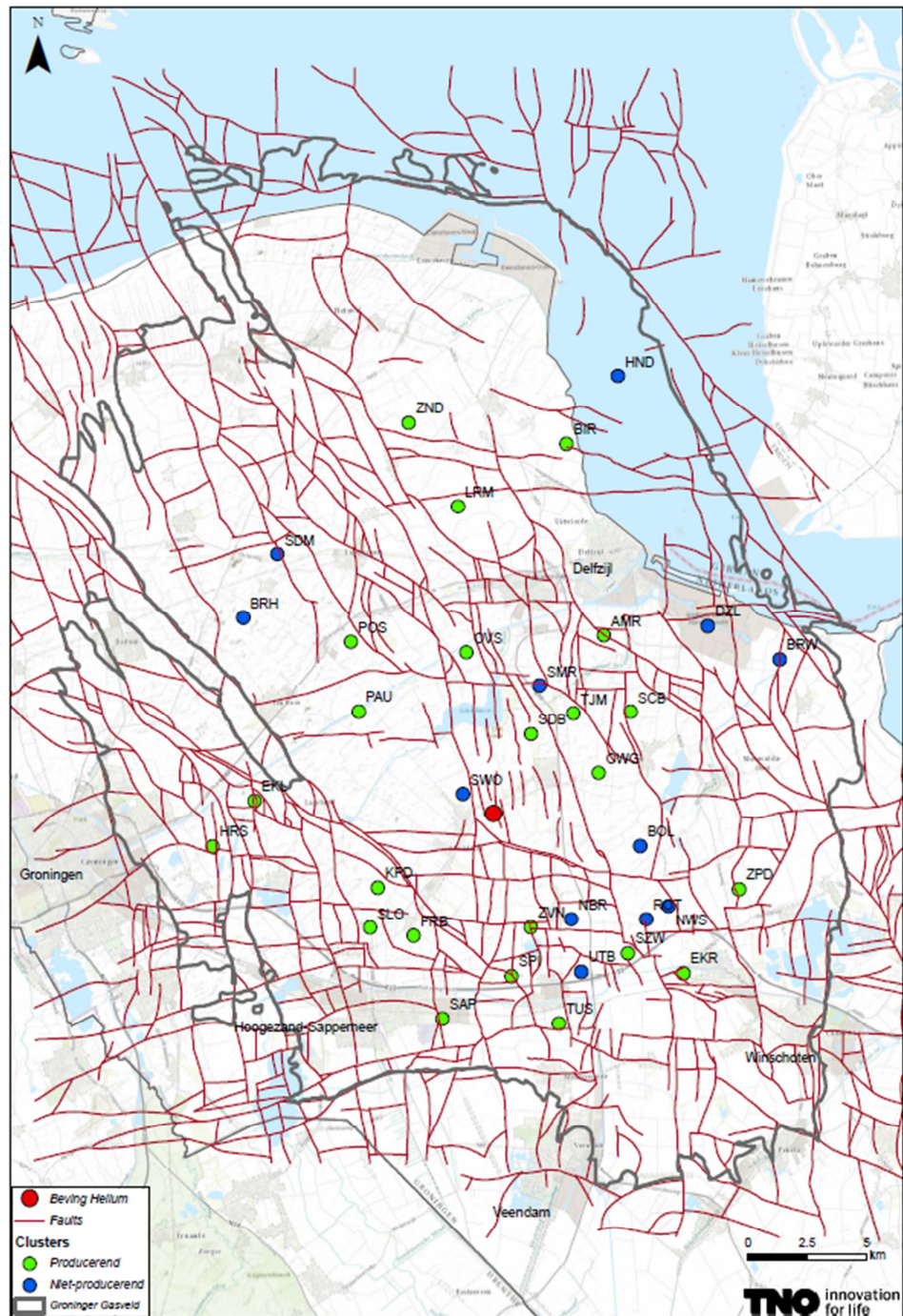


Figure 2-5. Location of the event near Hellum (red) with respect to the producing clusters (green) and the faults of the static geological model (dark red lines).

On September 30th a seismic event with a magnitude of $M_L=3.1$ occurred near Hellum (Figure 2-5). As mentioned in NAM (2013) the seismicity (number of events and magnitude) of the Groningen field is expanding in time over the field. The higher magnitude events occurred first in the center of the field (from 1991). As time progressed the larger events start to spread out from the center. This specific event is the most southern location of all $M_L>3.0$ events and fits in the trend of spreading seismicity.

In TNO (2014a) an increase in compaction and seismic moment release was calculated for a scenario where production in 2014 was limited to 42,5 bcm, and 40 bcm/year for 2015 and 2016. As Figure 2-6 shows the Hellum event took place in a location where an increase in compaction was calculated and subsequently an increase in potential seismic moment with a factor of about 1.6 (period 2014 to 2017).

Production in 2014 has been 42,4 bcm and production has been limited to 30 bcm for 2015. In this area of the field, production has generally increased since January 2014 (Figure 2-7 and Figure 2-2) to balance the production reduction in the center of the field. This increase was taken into account in the scenario of TNO (2014a). The production reduction in the southwest since January 2015 (Figure 2-1, Figure 2-7a) was not taken into account in the scenario of TNO (2014a). The production of clusters close by the event (Siddeburen (SDB), Tjuchem (TJM), Oudeweg (ODW) to the northeast and Kooipolder (KPD), Slochteren (SLO) and Froombosch (FRB) to the southwest) are moderately affected by the production reduction since January 2015 (see also Figure 2-7a and Figure 2-1). The clusters Oudeweg (ODW), Tjuchem (TJM) and Siddeburen (SDB) show an increase of production from July/August to September 2015 (Figure 2-7).

Please note that a single event (such as the Hellum event) is not able to demonstrate the validity or quality of any prognosis. Note also that the validity of the 2014 prognosis of potential seismic moment (Figure 2-6) depends on the future production profile.

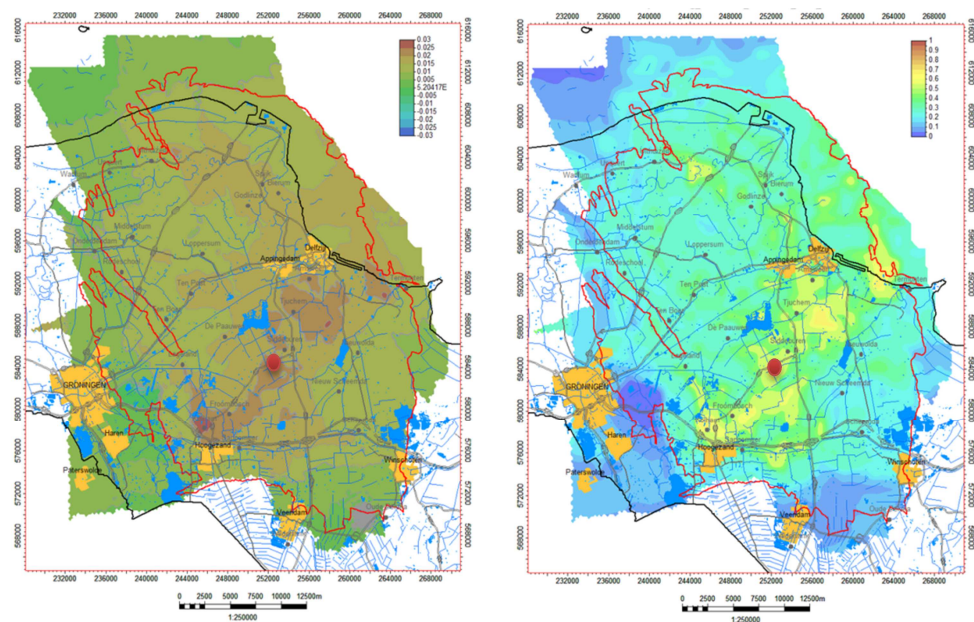


Figure 2-6. Increase in compaction and increase in potential seismic moment in 2014-2017 (The value 1.0 indicating a doubling of potential seismic moment which could be released, taken from TNO (2014a, Figures 6-2 and 6-4). The location of the Hellum event is indicated in red.

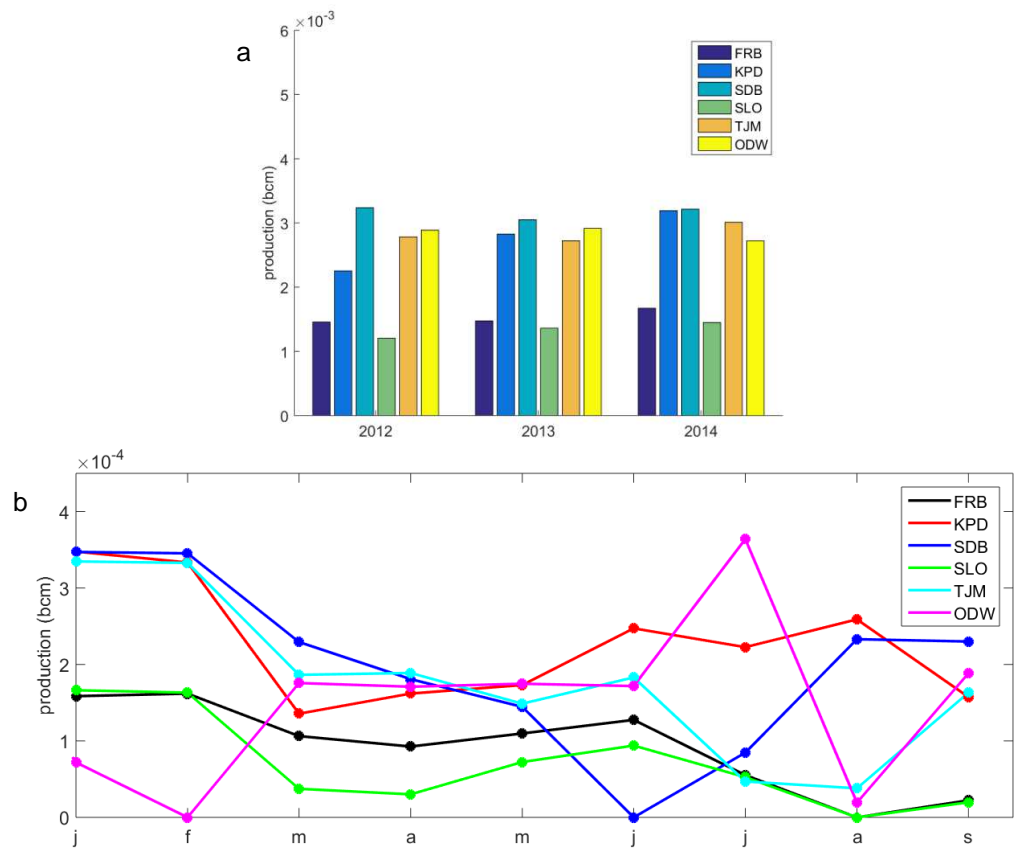


Figure 2-7. Production of clusters (FRB, KPD, SDB, SLO, TJM, ODW) yearly from 2012 to 2014 (a) and monthly in 2015 (b).

2.3 Event density maps

Figure 2-8 shows the event density for the period July 2012 to July 2015. The event densities were determined using a Kernel Density (standard GIS application) with a radius of 5 km and a cell size of 50 m. In January 2014 production was reduced in the center of the Groningen field. Since an expected effect on the seismicity would only show after a couple of months, a period from July up to July is chosen to show the seismicity since the production reduction in January 2014. Comparing July 2013 – July 2014 with July 2014 - July 2015 a reduction of event density can be observed in the center of the field. In general, event densities are lower from July 2014 to July 2015.

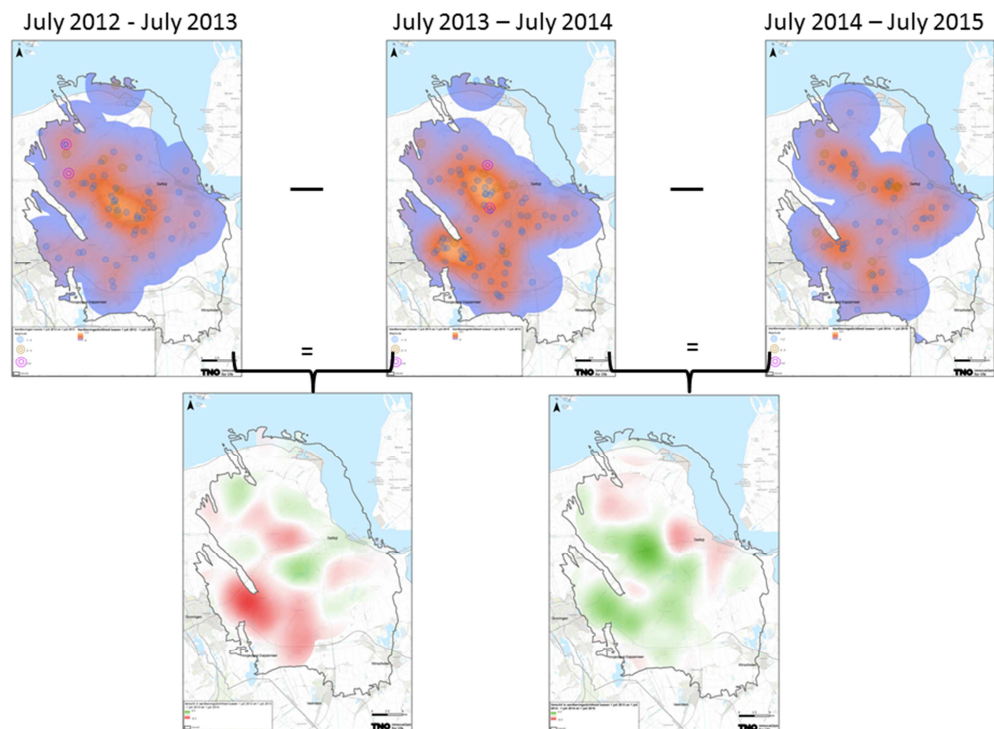


Figure 2-8. Top: Event density (number of events per km²) from July 2012 to July 2015. The observed events and their magnitudes are indicated by the colored small circles. Bottom: Difference in event density between the indicated periods. A negative (green) difference indicates a lower event density in the later period compared to the earlier period. Larger size figures are in appendix B.

2.3.1 Movie

TNO has made a movie of the event density per year (<http://www.nlog.nl/nl/hazards/subsidence.html>). In this movie event densities are shown looking back over the past year as indicated in the movie. The movie also shows an increasing event density up to 2014 (shown in the movie as JAN 2014 = event density from January 2013 to January 2014) and a decreasing event density after January 2014.

2.4 Visualization of events and production

If there is a relation between production and seismicity, where seismicity reacts on production changes with a certain delay, this should be visible in the data. In this paragraph we compute the moving sum of production and the number of seismic events to evaluate a relation between production and seismicity. First on a yearly basis for the whole field, then on a half-yearly basis.

The moving sum of production/number of seismic events is calculated as follows:

- Take the sum of 12 consecutive months of production/number of events.
- The result is displayed at the end of the time series.
- Shift the time period analysed by one month forward.
- Go to the first step until the end of the analysed period is reached.

The moving sum suppresses fast (e.g. seasonal) variations and brings forward more gradual changes in time. The yearly number of events above a certain magnitude is shown in Figure 2-9. The yearly sum of events with magnitudes above $M_L=0.0$ is almost equal to the yearly sum of events with magnitudes above $M_L=0.5$ since few events between $M_L=0.0$ and 0.5 are registered. Clearly the number of events per year increases which is especially evident for the smaller events, but also visible for all $M_L > 1.5$ events.

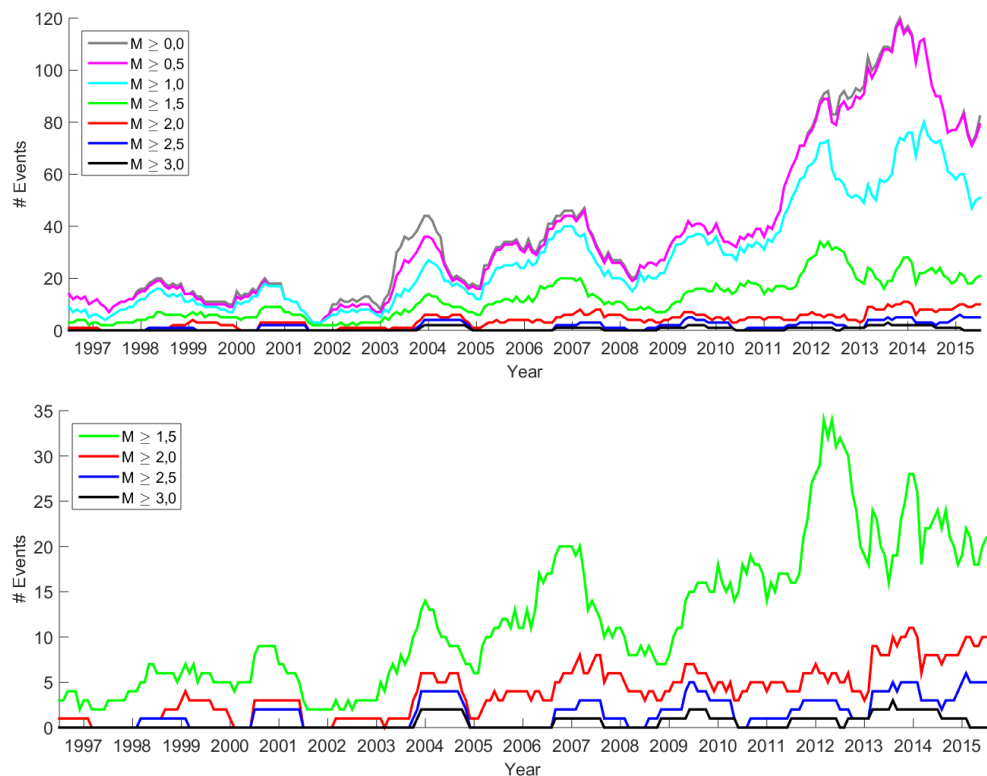


Figure 2-9. Moving sum of the yearly seismicity with magnitudes larger than specified magnitude; number of events indicated at i.e. January 2015, is the total number of events between 1st January 2014 and 1st January 2015. The difference between the figures is the magnitudes and the range of the number of events.

As indicated in TNO (2015), the seasonal variation in production is visible in the occurrence of seismicity with a delay of 5 and 7 months. Therefore the moving sum of yearly production is combined with the delayed sum of yearly seismicity. In Figure 2-10 and Figure 2-11 the production and seismicity are shown for all events with $M_L \geq 1.0$ (Figure 2-10) and $M_L \geq 1.5$ (Figure 2-11). Especially for the $M_L \geq 1.0$ events, there is a clear correlation between production and seismic events as from 2002/2003. Production changes are followed by seismicity changes a few months later. The correlation is also visible for the events with $M_L > 1.5$ but not as clear due to the decrease in the number of events available in this category. Visually in the period before 2002/2003, the production changes (3 maxima's) are not followed by seismicity changes (1 maximum). This does, however, not necessarily mean that production changes are not followed by seismicity changes in this period because other effects (e.g. criticality of the fault system, localization of the events) could be present.

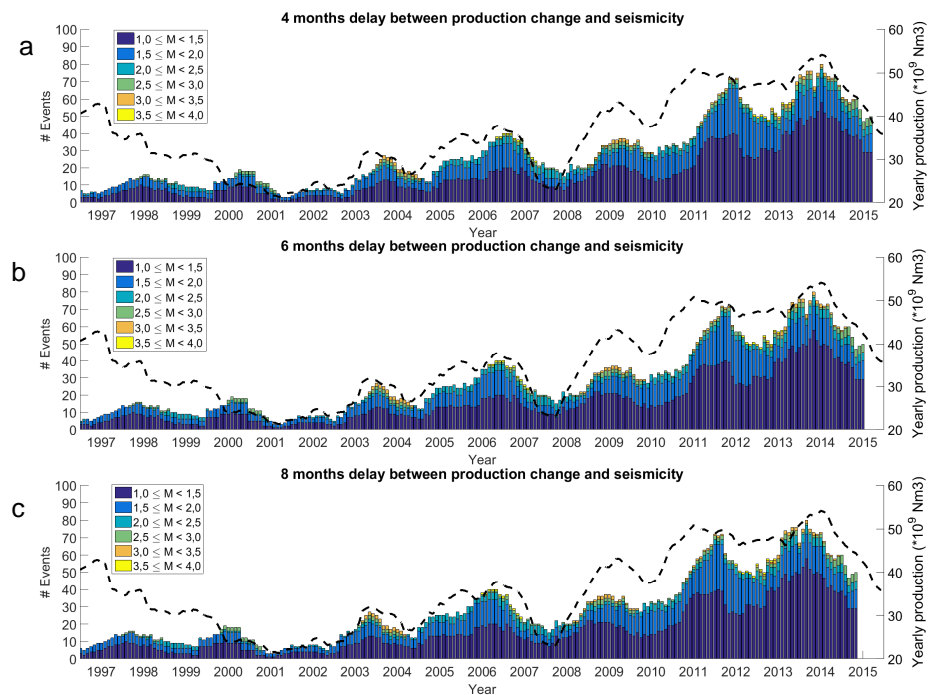


Figure 2-10. Moving sum of yearly production and yearly seismicity (all events from $M_L > 1.0$) using a delay between production and seismicity of 4 (a), 6 (b) and 8 (c) months.

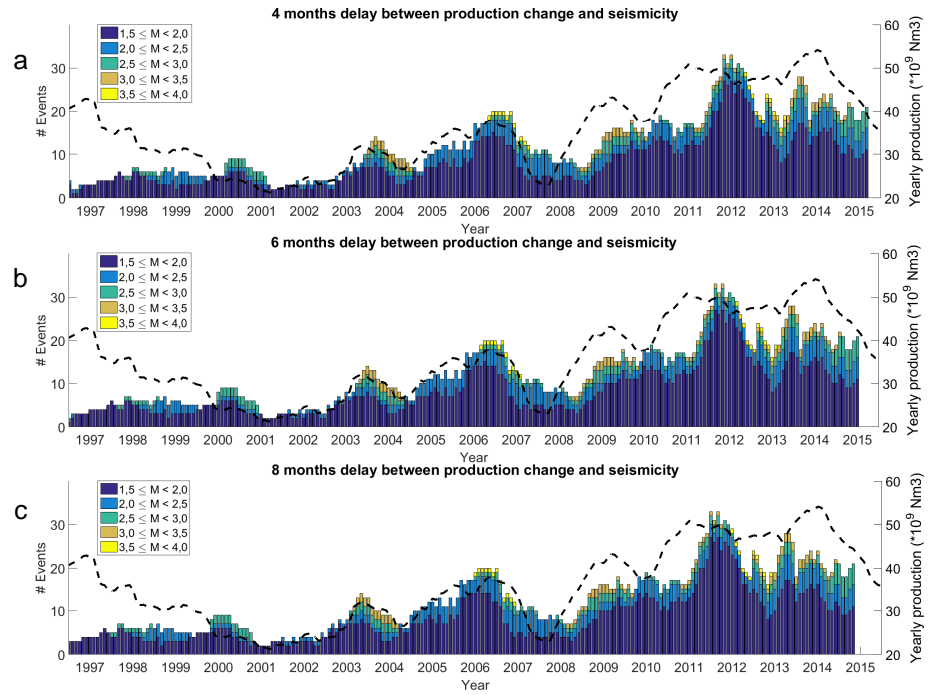


Figure 2-11. Moving sum of yearly production and yearly seismicity (all events from $M_L > 1.5$) using a delay between production and seismicity of 4 (a), 6 (b) and 8 (c) months.

Figure 2-12 and Figure 2-13 show the same relation for a half-yearly moving sum. Visually there is a clear seasonality in both the production as well as the seismicity. It is difficult to match individual peaks in production to peaks in the number of seismic events.

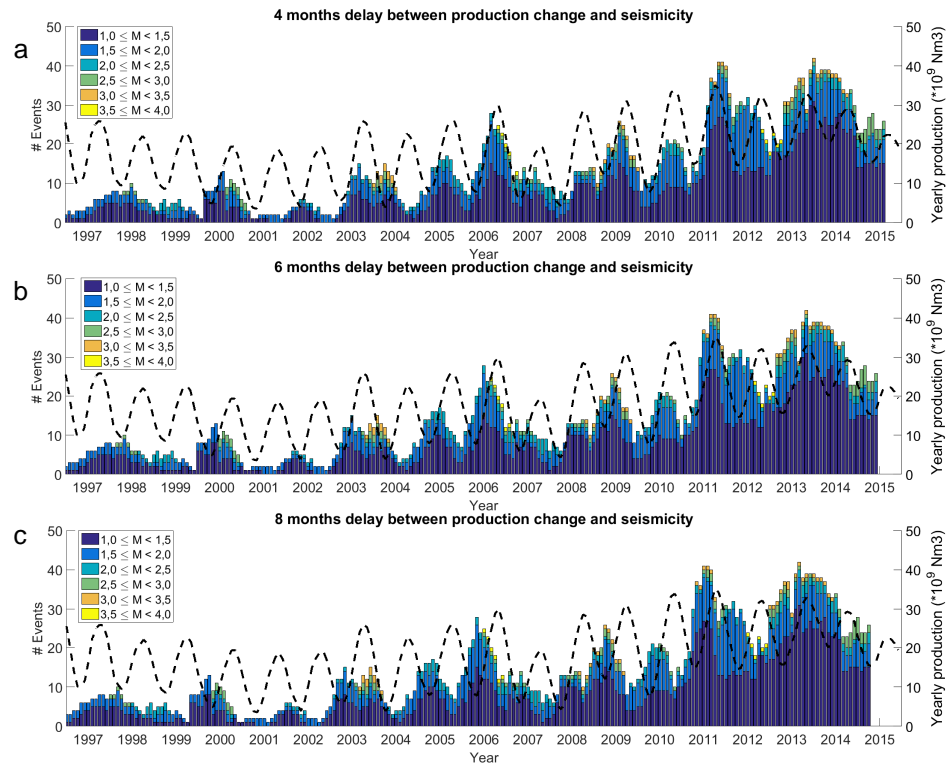


Figure 2-12. Moving sum of half-yearly production and half-yearly seismicity (all events from $M_L \geq 1.0$) using a delay between production and seismicity of 4 (a), 6 (b) and 8 (c) months.

2.4.1 Relation between production and seismicity?

If we assume that there is a physical relation between production and seismicity then the delay depends on the diffusion time of gas in the reservoir. Specific wells with production changes and their respective distance to the central fault system (in the Loppersum area) - since this area had most seismic events - would determine the diffusion time and, therefore, also the delay. In January 2014, production was reduced in the five central clusters of the field, which according to this visual inspection corresponds to a seismicity decrease with a delay of four months (Figure 2-10a). A pressure wave would take a shorter period to reach the central fault system from these central wells than from a more southern well which may be the reason that only a small delay is visible.

From this visual inspection no firm conclusions on the relation between production and seismicity can be drawn, although the observations do support such a relation.

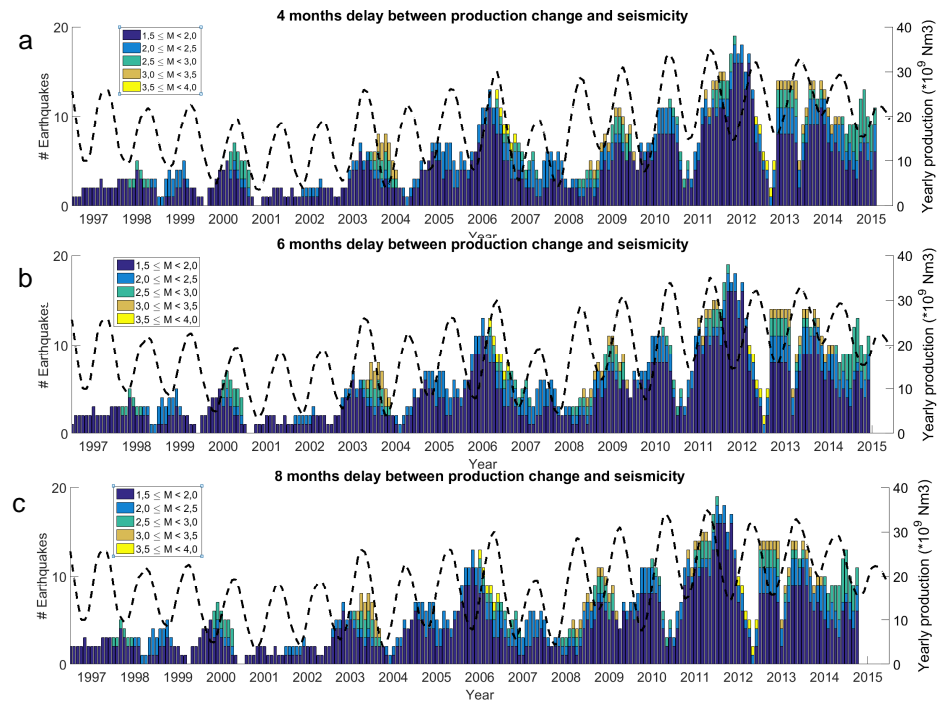


Figure 2-13. Moving sum of half-yearly production and half-yearly seismicity (all events from $M_L \geq 1.5$) using a delay between production and seismicity of 4 (a), 6 (b) and 8 (c) months.

3 What do we know about the statistical relation between production and seismicity?

In this chapter we review what we know about the relation between production and seismicity of the Groningen field. In the past (TNO 2014b; TNO 2015a) we have performed statistical analysis which are updated in this chapter using an updated seismicity catalogue (up to September 5th 2015) from the KNMI. The magnitude for which the catalogue is complete (period 1996 - now) over the Groningen field is somewhere between magnitudes $M_L=1.0$ - 1.5 (KNMI 2012, Pijpers 2015). The statistical analyses in this chapter use $M_L \geq 1.0$ unless otherwise mentioned. This may be a bit low as KNMI (2012, Figure 2b) indicates that in some areas of the Groningen field magnitudes $M_L=1.0$ - 1.5 are detected but not localized. The observed number of events is such that from $M_L \geq 1.0$ more events are available for statistical analysis.

The catalogue of seismic events has first been declustered. The algorithm of Reasenberg (1985) is used for the declustering. This is a deterministic algorithm, where each event is classified either as a mainshock or as an after- or fore-shock. The method identifies aftershocks by linking events to clusters according to spatial and temporal interaction zones. The temporal zone is based on Omori's law (for example Schcherbakov 2004), while the spatial zone depends on the stress distribution near the mainshock. The fore- and aftershocks are identified within one and ten days from the original event and the effective lower magnitude cutoff for the catalogue is chosen at $M_L=1.0$. In this way only independent events are used in the analyses. In the catalogue, 611 seismic events with magnitudes above $M_L=1.0$ are present (Figure 3-1a). After declustering, 594 seismic events are left in the same period (Figure 3-1b). From Figure 3-1 a change from a more or less constant number of events per year to an increasing number of events per year can be seen around 2003. The significance of this change is evaluated using the Bayesian change point model in the next section.

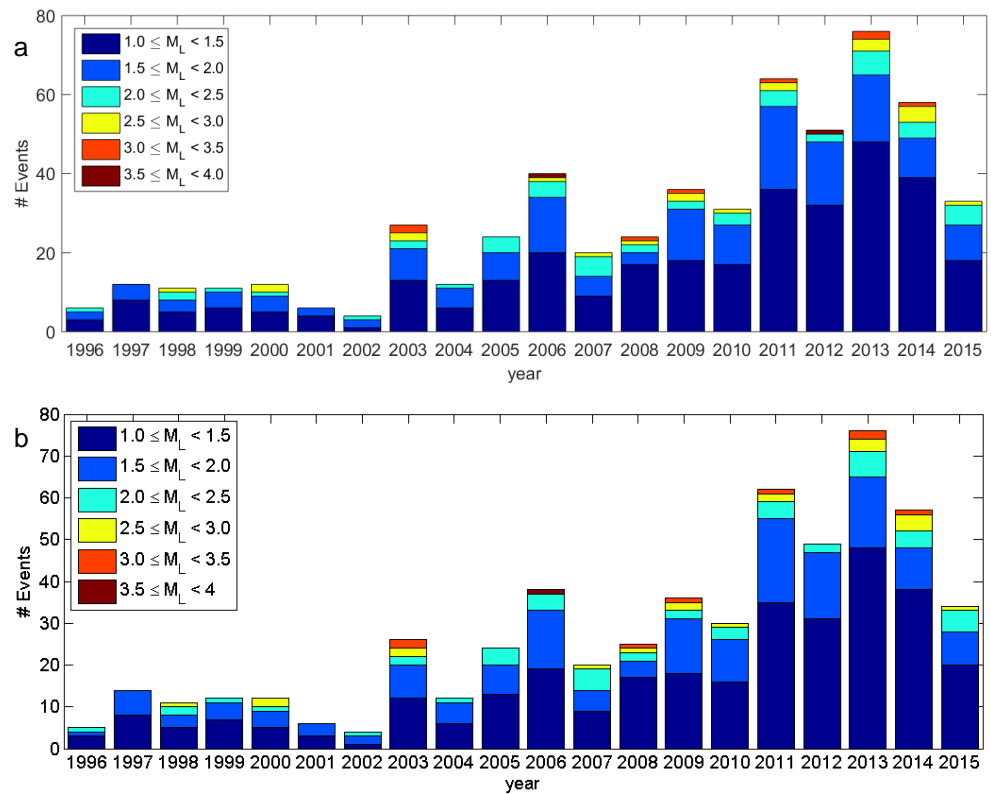


Figure 3-1 Number of events occurring within the contour of the Groningen gas field as a function of time from 1996 and Magnitude (M_L) for the whole catalogue (a) and the declustered catalogue (b).

3.1 Bayesian change point model

For an introduction on the Bayesian change point methodology we refer to TNO (2014b, 2015a). From the declustered seismicity database, only the events with magnitudes larger than $M_L \geq 1$ within the contours of the Groningen field were selected. For the analysis a point in the center of the field (latitude 53.297 and longitude 6.782) and a radius is defined, such that all induced events related to the Groningen gas field are selected for the analysis.

The models we compare in the Bayesian change point analysis are stationary, meaning that event rate is constant. Two models are compared: one has a constant event rate during the entire observed time period $T=[0,t]$, while the other model has a constant rate before the change point and a different, constant rate after the change point. From the statistical analysis in TNO (2014b, 2015a), as well as from the simple visual inspection of the events in Figure 3-1, there is an indication that event rate changes with time. In the case of an increasing event rate (for example, Figure 3-2b), the Bayesian change point model will find a change point with a constant rate before and after (Figure 3-2a). To check whether we are dealing with situation in Figure 3-2a or b, we will perform the Bayesian point change analysis for different time intervals.

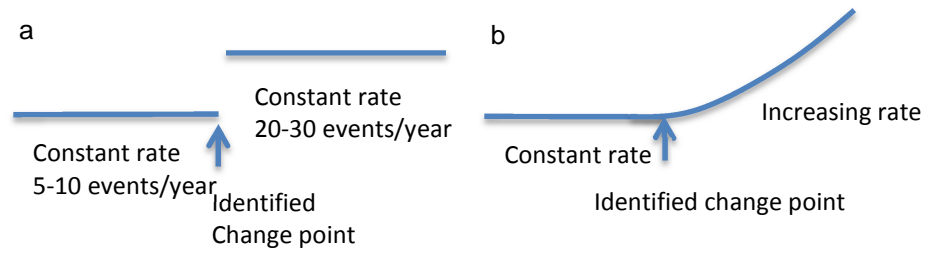


Figure 3-2. Illustration of the Bayesian change point model in the case of a single step increase (a) or an increasing rate with time (b).

Table 3-1. Overview of investigated time intervals and the resulting change points in event rate. The Bayes factor determines the odds of change point model above one single constant rate model.

Time interval	Pre rate (events/year)	Change point (CP)	Post rate (events/year)	Bayes factor
T ₀ : 1991 - 1.1.2004	~ 9	Dec 2002	~ 23	79
T ₁ : 1991 - 1.1.2011	~ 9	Dec 2002	~ 28	5.74*10 ¹¹
T ₂ : 1991 - 1.1.2012	~11	Oct 2004	~ 32	1.28*10 ¹⁸
T ₃ : 1991 - 1.1.2014	~12	Jan 2005	~44	1.43*10 ³¹
T ₄ : 1991 - 5.9.2015	~16	Oct 2008	~51	1.92*10 ³⁸
T ₅ : 15.11.2012 - 05.09.2015	~73	May 2014	~47	15

The first change point is identified on December 31st, 2002. The accuracy of this change point is about one month. The event occurrence rate has increased from 9 events per year to about 23 events per year (Table 3-1 and Figure 3-3a). For longer time intervals (up to January 1st 2011), the identified change point is still December 31st 2002, but the post event rate increases to about 28 events per year (Table 3-1). Post event rates increase with investigated time interval for the same change point.

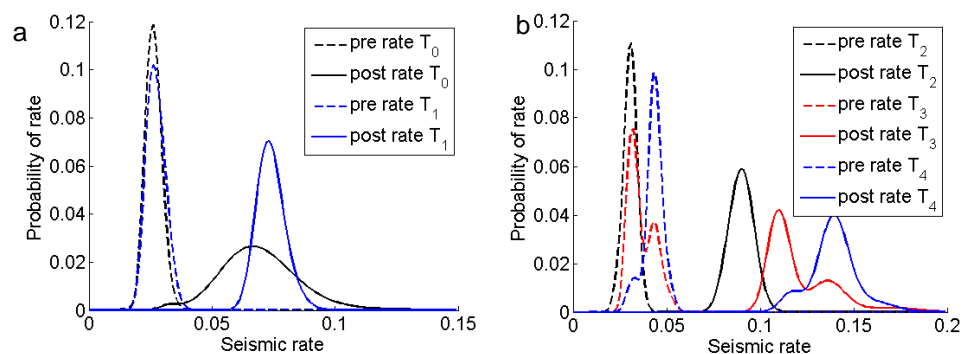


Figure 3-3. The pre and post date change event rates for time intervals T₀ and T₁ (a) and T₂ to T₄.

The Bayesian change point analysis supports the earlier observation that event rates are increasing after 2002. A Bayesian change point model with an increasing rate after the change point would be more appropriate in this case. The Bayes factors found are high (>10¹⁰) which indicates that this change point model is fully supported by the data.

A schematic representation of the number of events occurring in Groningen (up to 13th august 2015), and 2 different change points (for time interval T1 and T4) with the respective pre and post event rates are shown in Figure 3-4. Estimated rates correspond well to the observed number of events.

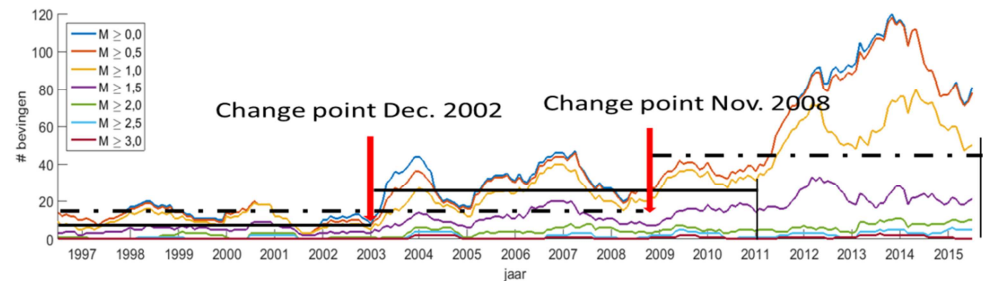


Figure 3-4 Illustration of the relation between the Bayesian point change analysis and the number of events per year from the Groningen seismicity catalog (from Figure 2-9). Change points for time intervals T1 and T4 and corresponding pre and post event rates are shown.

3.1.1 *The period after January 2014*

Gas production has been reduced since January 2014. In this paragraph we analyse the seismicity catalogue with the Bayesian change point model to see whether seismicity has changed significantly since January 2014. For the time interval T_5 (November 2012 – September 2015), a change point is found in May 2014. We selected this time interval on the value of the Bayes factor (at least 10) and the number of events available. For this change point, a decrease in seismic event rate is found (Figure 3-5). The event rate before May 2014 is around 70 events per year and decreases to about 45 events per year after the change point. In this case only a small time period (January 2014 to September 2015) is used for the analysis. Seasonal effects (section 2.4.1. and 3.3) may play a large role here. These values could, therefore, be modified if a longer time period is taken in future analyses. The probabilities of the pre and post rate overlap (Figure 3-5), indicating that this difference in event rate is not highly significant yet. Figure 3-5b shows the probability distribution of the change point in time. In comparison to the other identified change points, this probability distribution is broader, ranging from March 2014 to June 2014, with the highest peak in May 2014.

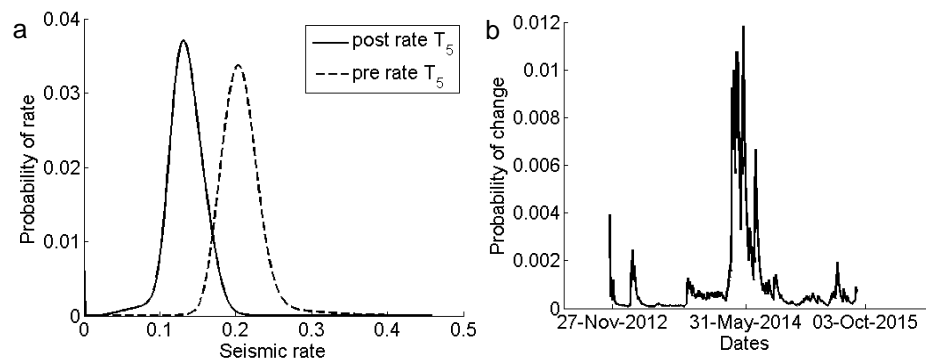


Figure 3-5a. The pre change date event rate (in events/day) – dashed line and the post change date event rates (in events/day) for the change point on May 19th 2014 and b. The probability of change in time over the period of 2012 up to now (Sept. 2015).

Note: the probability density function of change point time (in Figure 3-5b) is calculated from the marginal posterior distribution of change time, and converted to probability by dividing the values for each day by the sum of values for all days in the observation period, such that the sum of probabilities equals one. Absolute values of probabilities are rather small since there are, in this short observation period, already 1015 days and the mean probability is 0.0009. This does not make the result statistically less significant.

3.2 Bayesian Model comparison

In TNO (2014b) the Bayesian Model comparison was introduced. In this model three basic trend models were compared: a Poisson distribution with a constant, an increasing, and a decreasing seismic event rate.

The model comparison is actually quite similar to the Bayesian change point model, the difference is in the non-constant event rate and no change point. The results of the Bayesian Change point model, i.e. event rate is increasing with time, give the rationale of using a Bayesian model comparison with an increasing rate. The Poisson models were compared to each other in three different parts of the Groningen field: The Center, Southwest and Other area (TNO 2014b). In these areas the seismicity database of the KNMI was updated up to September 2015 and declustered using the Reasenberg (1985) algorithm. The analysis showed a preference for a constant seismic event rate before January 2003 and a strong preference for an increasing seismic event rate in the period from January 2003 to January 17th 2014 for all three areas of the Groningen field. This supports the findings of the Bayesian change point model in the previous section of this report.

3.2.1 *The period after January 2014*

For the period after January 17th 2014 it was concluded (TNO, 2015) that the data slightly favor a decreasing trend for the seismic events but that data was too sparse to come to a firm conclusion. This conclusion is still valid for the seismic database up to September 2015 (Table 3-2 and Table 3-3). However, the decrease model is favored more than in the previous results of TNO (2014b), i.e. the Bayes factor has become larger (Table 3-3).

Table 3-2. Bayes factors and number of events for the model comparison between a stationary event rate and an increasing event rate. Data since 17th January 2014

Name	Bayes Factor Increase/Stationary	Number of events
Adapted Central	0.92	16
SW	0.61	20
Other	0.61	42

Table 3-3. Bayes factors and number of events for the model comparison between a stationary event rate and an increasing event rate. Data since 17th January 2014

Name	Bayes Factor Decrease/Stationary	Number of events
Adapted Central	0.88	16
SW	2.74	20
Other	1.52	42

In order to strengthen the results, in TNO (2015) an alternative approach was taken. The data are divided in segments of 1000 days and we looked at a *constant rate model for each segment*. This simplifying assumption is reasonable on account of the timescales of change found in earlier analysis (TNO 2014b).

Table 3-4 indicates the number of events in the different areas in the Groningen field for time spans of 1000 days since the first occurring event in 1991 updated since TNO (2015). Table 3-5 shows the event rate including standard deviations. From these results we conclude:

- In the Central (C) area the event rate has gone down significantly (four standard deviations).
- In the Southwest (SW) area the event rate has gone up significantly (two standard deviations).
- In the Other (O) area the event rate has gone down significantly (two standard deviations).

We remember the reader that the preference of a decrease model with the two parameters "a" and "tau" (TNO Report 2014b) only states that the event *rate* diminishes, but says nothing about the "best" value of the constant "a" in the model. We see that the event rate in SW has gone up, that is the best value of "a", The Bayes Factor nevertheless indicates that this rate seems to diminish after January 2014 (Table 3-3).

Table 3-4. The number of events with magnitude $M_L \geq 1.0$ in the regions Central (C), Southwest (SW) and Other (O) as a function of the number of days since the start of observed seismicity on December 5th 1991.

Time (days)	Events $M_L \geq 1.0$		
	C	SW	O
1 – 1000	7	2	20
1001 – 2000	7	0	14
2001 – 3000	12	5	17
3001 – 4000	7	3	11
4001 – 5000	29	7	23
5001 – 6000	31	12	28
6001 – 7000	31	10	49
7001 – 8080	63	19	106
8081 – 8670	16	20	42

Table 3-5. The event rate, including standard deviation, in the regions Central (C), Southwest (SW) and Other (O) as a function of the number of days since the start of seismicity on December 5th 1991.

Time (days)	Event rate		
	C	SW	O
7000 – 8080	21/year \pm 2/year	6/year \pm 1.5/year	36/year \pm 4/year
8080 – 8670	10/year \pm 2/year	12/year \pm 3/year	26/year \pm 4/year

3.3 Seasonality

As production follows the summer-winter cycle production exhibits seasonal dependence. The question is whether seismicity shows seasonal dependence as well.

In TNO (2015) correlation functions were used to investigate and illustrate seasonality in production and seismicity. The autocorrelation of production confirmed a clear seasonal dependence of production. Since gas production in Groningen, in the past, has had higher production in the winter seasons, a seasonal dependence in the production numbers is obvious. The cross-correlation between production changes and the number of seismic events showed a maximum positive correlation after 5-7 months, 17-19 months and 29-31 months. Figure 3-6 shows the yearly normalized correlation between production changes and seismic events for the period between 2006 and 2014. Most years show seasonal correlations (especially 2006, 2009, 2010, 2011, 2012, 2014). A notable exception to this is the year 2013 where seismicity does not show seasonal variations.

Earlier (TNO 2015) we have chosen to focus on the whole seismicity catalogue. One might argue that since not all magnitudes can be registered over the entire field, a seasonality check on all magnitudes may suffer from bias. It is worthwhile to see whether seasonality exists for larger event magnitudes ($M_L \geq 1.0$ and $M_L \geq 1.5$). Figure 3-7a shows the stacked correlation function between seismic events and production over the whole period of 2003 to 2012 for different ranges of seismicity data. If only the events with magnitude larger than $M_L \geq 1.0$ and $M_L \geq 1.5$ are chosen the correlations are smaller in magnitude but still present.

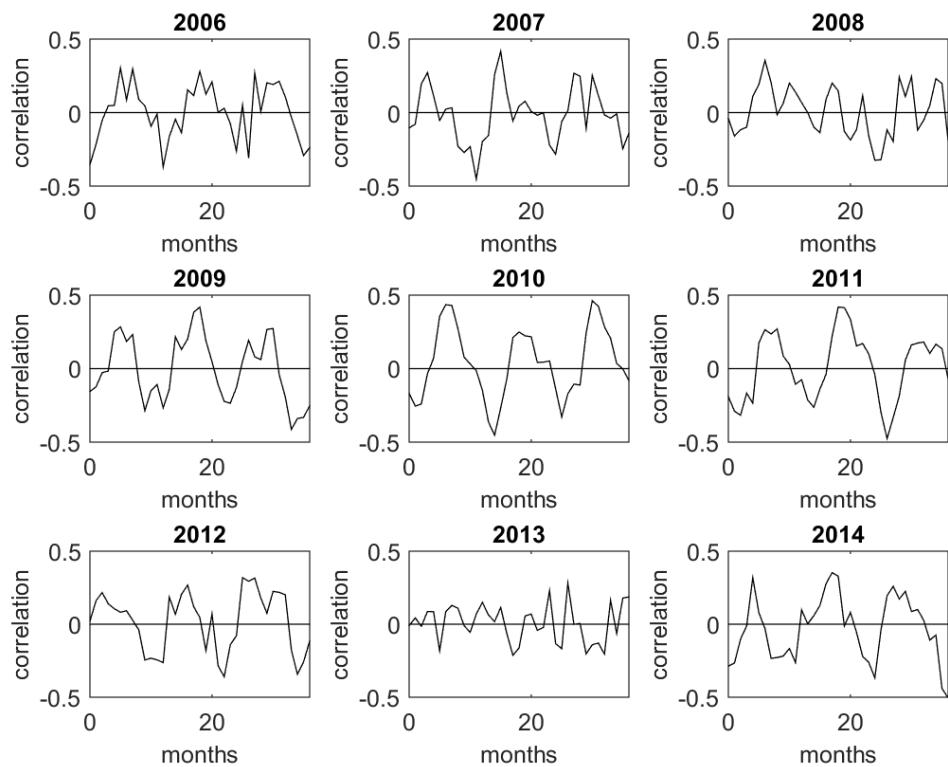


Figure 3-6. Correlation per year for all magnitudes above $M_L=1.0$.

Another effect that may have a bearing on our findings is the occurrence of foreshocks and aftershocks. Since aftershocks will be clustered around individual events, the seasonality might appear more pronounced than without aftershocks. As Figure 3-7b shows, even if declustering is applied to the KNMI seismicity database, correlations are still present and comparable to the correlations found without declustering.

This method demonstrates a seasonal effect in the seismicity. The delay between the production seasonal effect and the seismicity seasonal effect is typically 5-7 months. As is well-known, correlation in itself does not prove causality. The case for causality must be made by introducing a cogent physical mechanism between the agents whose correlation is established. In the case under study we do have a plausible mechanism in a *varying pressure in the reservoir* as a result of production variation. Furthermore, the lag between production change and seismicity change is of the order of months. This fits in with pressure travel times over ranges of several kilometers, as shown in TNO (2014, Appendix A). Hence, we have a case that production changes, at least in part, cause the observed seasonality in the event rate.

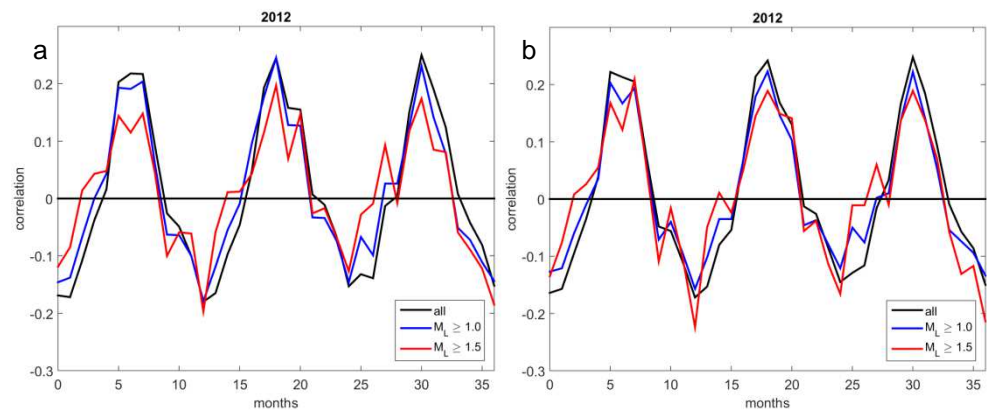


Figure 3-7. The stacked correlation in 2012 between production on a monthly basis and the number of seismic events for all magnitudes of the seismic catalogue (source: KNMI), for magnitudes larger than $M_L \geq 1.0$ and for $M_L > 1.5$ (a) and same for the declustered catalogue (b).

A final remark on the *strength* of the correlation is in order. In normalizing the cross-correlation between production changes and events (see Appendix A) we discovered that the numerical values lie between -0.4 and +0.4 (Figure 3-6). In order to get a feel for the strength of such a correlation we experimented with purely hypothetical situations where the event rate was purely constant or purely sinusoidal; we left the production data untouched. In the first case correlations were typically below 0.1 in absolute value; in the second case absolute values up to 0.8-0.9 could be seen (Figure 3-8). This suggests that the correlation we found has medium strength. Production *changes* are not the sole drivers of the seismicity, production history could perhaps play a role as well. Also the stacked signal (Figure 3-7) is smaller (between -0.2 and +0.2) indicating that stacking reduces the seasonal signal. This can be understood if we realize that different years have colder/warmer winters that start and end earlier/later and that therefore the production changes will not be exactly similar for each year. Also the seismicity occurring due to pressure changes in the reservoir will depend on which clusters have produced in the months previously and their distance to the major fault systems.

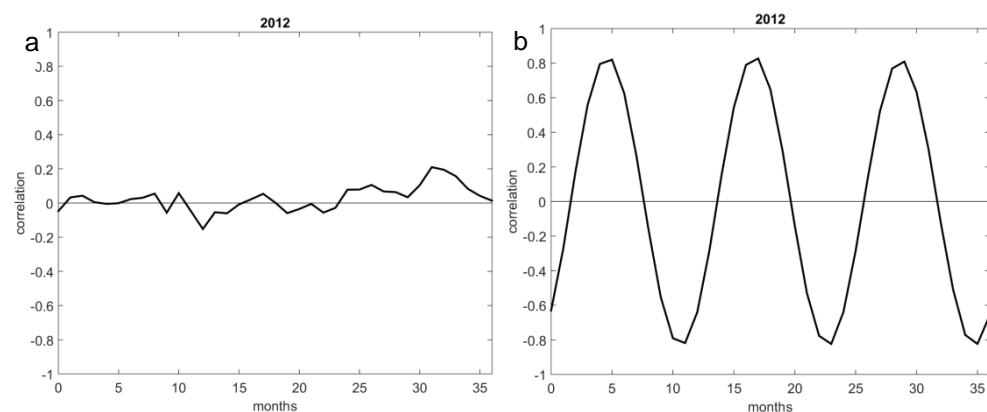


Figure 3-8. Tests of significance of correlation: test with a constant seismicity over the year (a) and test with a perfect sinusoidal behavior of the seismicity (b).

4 The causal relation between production and seismicity

The previous chapter shows that there is statistical evidence for a reduction in event rate since 2014, corresponding to a production reduction of the field. Statistics, alone, cannot prove a causal relation between production and seismicity. For instance, there is a statistical relation between the number of storks and the child birth rate, but this does not mean that there is a physical relation between the number of storks and the birth rate. “Proof” of causality requires physics. In this chapter the physical relation between production and seismicity is examined using geomechanical modelling of a single fault in a synthetic reservoir. Qualitative conclusions are drawn for the Groningen field case.

4.1 Numerical model for rupture of a single fault

Geomechanical numerical models for rupture (e.g. Wassing et al., 2014) allow to investigate the process of mechanical rupture and associated seismic moment evolution. In such models, the fault is discretized in small patches. As production of gas takes place, stresses on the faults are affected. In the case of normal faulting, which is dominantly present in the Netherlands (including the Groningen field), gas production will lead to an increase of stress relative to the yield criterion. If one patch fails due to increasing stress to the yield criterion, the patch will slip. This results in lowering the out of balance stress.

From lab experiments it is well known (cf. Niemeijer and Spiers, 2007) that upon slip the friction angle of the slipping portion of the fault is reduced, which may explain seismic activity in reservoirs.

The slip of the patch destabilizes stresses in the surrounding patches, which in turn can start to slide. This can be considered as a domino effect in which the height of the dominos is given by reduction of friction angle through slip (also called stress drop) and the spacing between the dominos by the stability of the in situ stress (how far it is from failure). If faults are critically stressed from the start of production, the dominos are close to each other, and create large rupture surfaces early in the depletion history. When the faults are not critically stressed the dominos are further apart and will only result in larger rupture areas after some period of depletion. The rupture surfaces tend to be restricted to that part of the fault area where compaction stresses build up.

4.1.1 *Model*

We illustrate these effects by rupture modelling of a simple fault geometry for a depleting gas reservoir, which is bounded by a steeply dipping fault, following the model setup of Van Wees et al. (2014). Figure 4-1 shows the adopted fault and reservoir geometry. We subdivide the fault in patches of 50x50m and apply a rupture model with a constant stress drop (through a drop in friction angle of 2 degrees). The fault surface is assigned by a slight natural roughness, preventing large portions of the fault to become critically stressed at exactly the same time. We

use a rectangular reservoir geometry with 2 x 2 km side length. The thickness of the reservoir is 150 m and the gas water contact (GWC) is at 2800 m depth. The initial pressure in the reservoir is 280 bar. The initial in situ stress has a vertical least principal stress, based on an overburden weight adopting a bulk rock density of 2.2 g/cm³. The reservoir is bounded on one side by a fault, dipping 70 degrees. The Coulomb stress change on the fault is modelled in 5000 time increments applying a linear pressure depletion resulting in a residual pressure of 5% of initial values. Mechanical properties, rock and fluid density are in agreement with Van Wees et al. (2014).

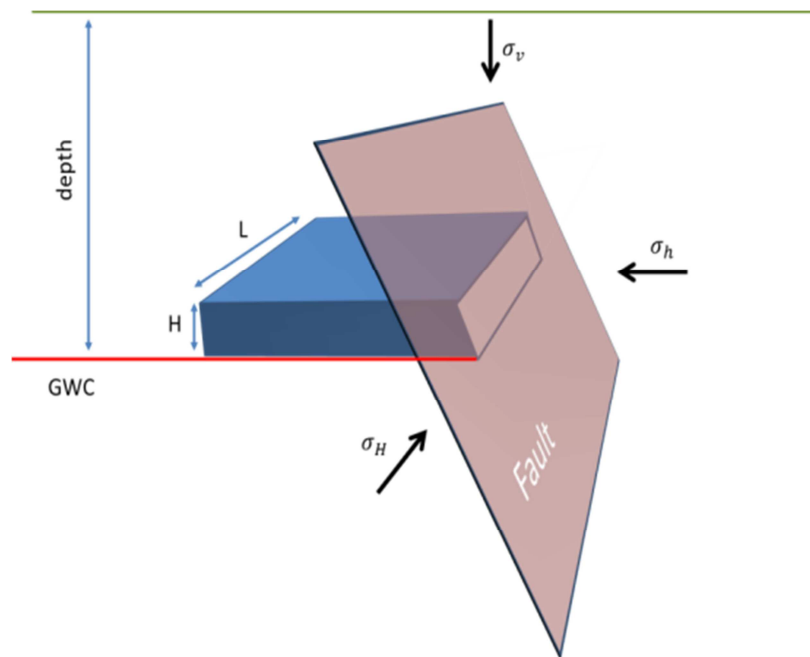


Figure 4-1 Model geometry (from Van Wees et al., 2014).

4.1.2 Results

Figure 4-2 and Figure 4-3 show the seismic events and cumulative seismic moment for an in-situ stresses which are critical (Figure 4-2) and subcritical (Figure 4-3) respectively. In the model, the seismic moment of each event has been calculated from the average of slip of the ruptured patches times the rupture area times shear modulus.

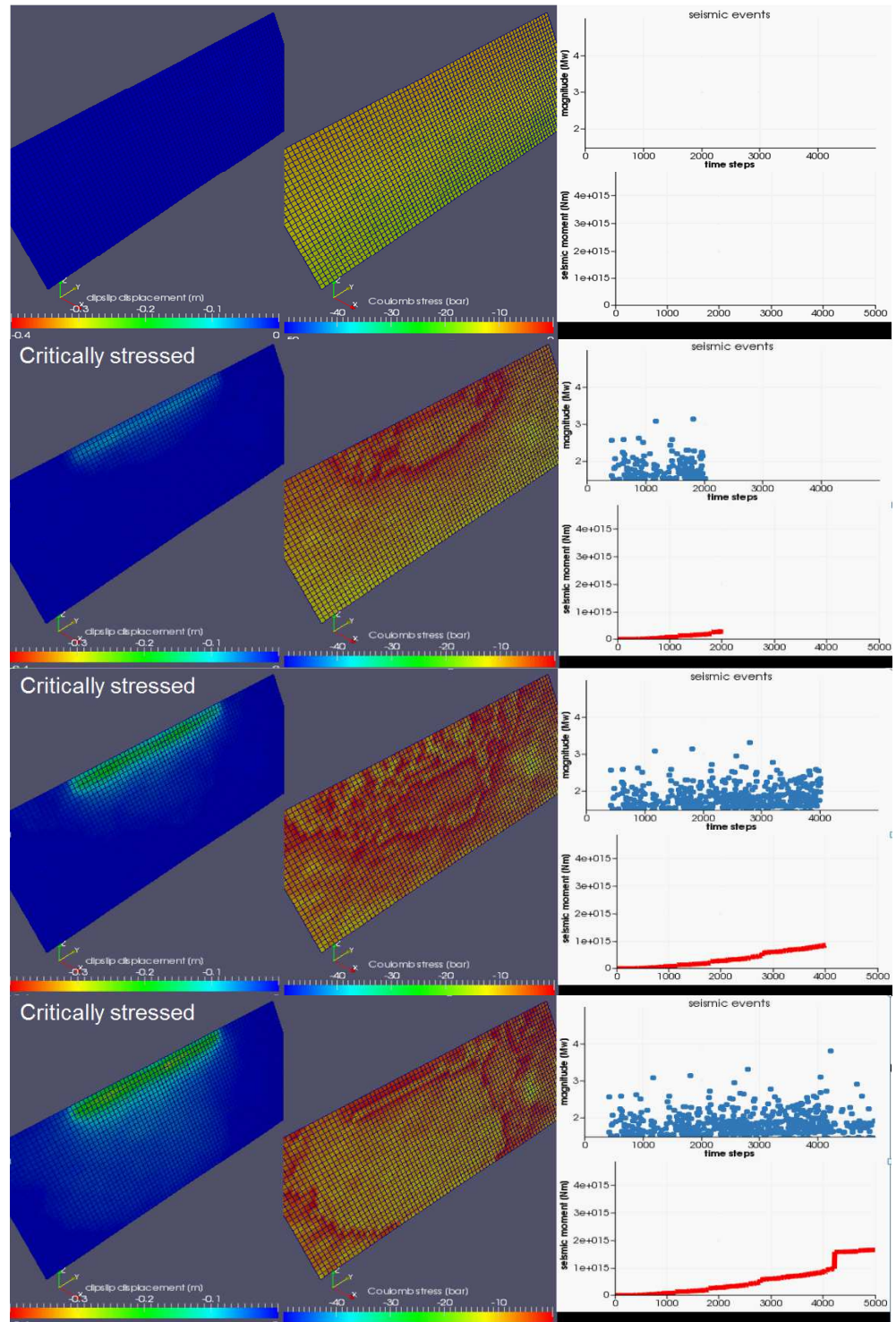


Figure 4-2 From left to right, displacement [m], Coulomb stress below failure criterion (red means fault should slip) and modelled seismic events (magnitude versus time on top and seismic moment versus time on the bottom), for in-situ horizontal to vertical effective stress ratio of 0.34. From top to bottom: initial situation, after 2000, 4000 steps and 5000 time steps. The in-situ stress on the fault is critical causing events after 10% of the reservoir depletion.

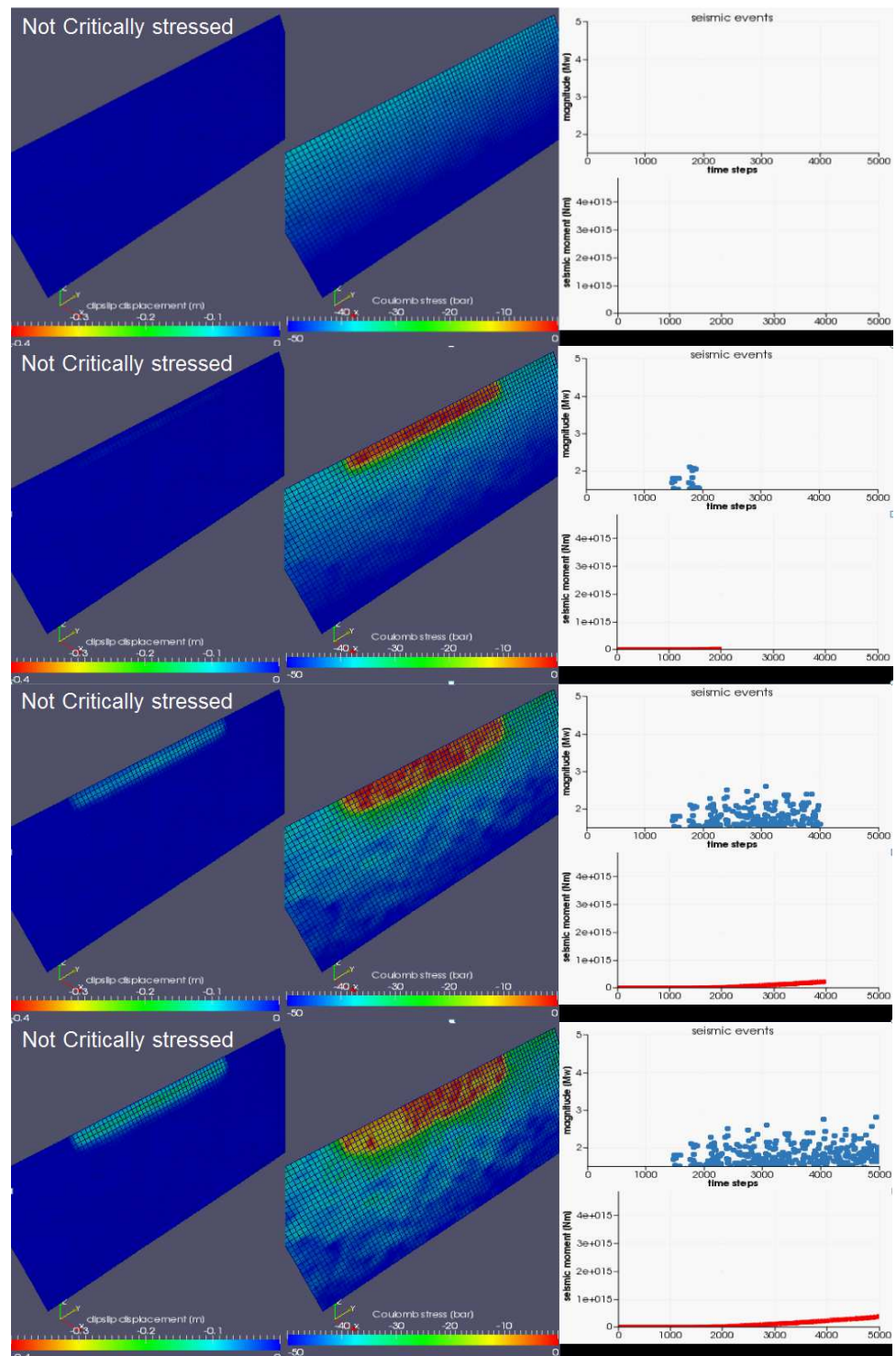


Figure 4-3 From left to right, displacement [m], Coulomb stress below failure criterion [bar] (red means fault should slip) and modelled seismic events (magnitude versus time on top and seismic moment versus time on the bottom) for in-situ horizontal to vertical effective stress ratio of 0.43. From top to bottom: initial situation, after 2000, 4000 steps and 5000 time steps. The in-situ stress on the fault is sub- critical causing events after 30% of the reservoir depletion.

4.1.3 *Relevance for relation between seismicity and production for the Groningen field*

The simple model highlights the strong sensitivity of the occurrence of events as a function of in-situ stress on faults. In the case of a critically stressed (or 'critical') fault, events occur almost immediately and their magnitudes are more-or-less the same over the whole time interval, i.e. the events can be described using a stationary Gutenberg-Richter equation. The highest magnitude corresponds to movement of the entire fault. In the case of a non-critical fault, events only occur after some time and there is a build-up in the magnitude of the events that take place, visible from time step ~1500 to ~2500. The latter situation corresponds to the Groningen case where seismicity was first registered in December 1991 while production was started in 1963. Also in Groningen, a build-up of seismicity has been observed, i.e. increasing event rates and increasing magnitudes which can be described by a non-stationary Gutenberg-Richter equation. Even though this model only has a single fault, the characteristics of the seismicity in Groningen are present. The geomechanical model indicates a direct relation between production and seismicity through stress increases on the faults in the reservoir.

5 Findings

State Supervision of Mines has requested the following technical evaluations from TNO-AGE:

- Effect of the production reduction on seismicity
- Update on the seismicity of the Groningen field

Response of induced seismicity to production changes in the Groningen field

The relation between production, faults and seismic events is studied using a three-step approach. The first step is visual inspection of the observations. As a second step statistical studies have been performed on the seismicity. In addition correlations between measured production and observed seismicity have been analysed. Statistics cannot prove causal relations. Hence, the third and last step is to check whether the statistical correlations are physically meaningful by applying a geomechanical model.

Visual inspection

In the period from 1996 to 2002/2003, the production changes (3 maxima's) are not followed by seismicity changes (1 maximum). Since 2002/2003 production changes are followed by seismicity changes with a delay of 4-8 months. Following the production reduction in January 2014, event densities show a decrease in the center of the field. Overall, event densities have decreased in 2014 and 2015 compared to earlier years.

Statistical analysis

The results show a statistical significant relation between production and seismicity within the framework of Bayesian analysis:

- a constant event rate up to ~2003,
- an increasing event rate from 2003 to 2014,
- in the center of the field a lower event rate from early 2014 to now,
- in the southwest of the field a higher event rate from early 2014 to now,
- seasonality in the number of seismic events, and a delay of 2 to 8 months between production changes and seismicity.

Fault model

Geomechanical analysis provides a physical, fault based mechanism between (changes in) production and seismicity. Modelling of a single fault in a synthetic reservoir demonstrates characteristics of the observed seismicity in the Groningen field.

Main finding

The effect of existing production measures (in particular those of January 2014) on seismic events has resulted in a decreased rate of seismic events in the center of the field in the period 2014 to September 2015. Please note that earlier work (letter AGE 14-10.016, accompanying report TNO, 2013) suggests that such an effect is temporary and also depends on the future production scenario (i.e. a lower production rate may extend the effect in time).

Update on the seismicity of the Groningen field September 2015

Due to the installation of additional borehole seismometers the number of observed, smaller events ($M_L < 1.0$) has increased considerably in 2015.

A limited number of $M_L > 2.0$ events have occurred, the largest of which was the event near Hllum ($M_L = 3.1$) on September 30th 2015.

In Groningen seismic events first occurred in the center of the field. Over time and with continuing production, $M_L > 1.5$ events are gradually spreading out from the center (NAM, 2013). The Hllum event occurred south of previous $M_L > 3.0$ events and fits in this trend.

Based on assumptions for a Groningen production profile from January 2014 to January 2017, TNO (2014a) prognosed compaction (as a proxy for potential seismic moment). Near the location of the Hllum event the assumed production profile is close to the actual production profile, especially in the year 2014. Prognosed potential seismic moment at this location is about 1.6 times higher in January 2017 compared to January 2014 (Figure B).

Please note that a single event (such as the Hllum event) cannot demonstrate the validity or quality of any prognosis. Note also that the validity of the 2014 prognosis of potential seismic moment (Figure B) depends on whether the actual production is similar to the assumed production scenario of TNO (2014a).

6 References

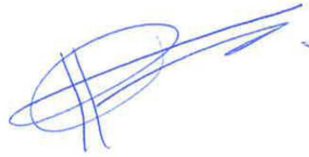
- EZ 2014 Brief van de Minister van Economische Zaken aan de Vaste Kamercommissie (kenmerk: DGETM/ 14008697), 17 januari 2014
- EZ 2015a Brief van de Minister van Economische Zaken aan de Vaste Kamercommissie (kenmerk: DGETM/ 15015030), 09 februari 2015
- EZ 2015b Brief van de Minister van Economische Zaken aan de Vaste Kamercommissie (kenmerk: DGETM/ 15086391), 23 juni 2015
- Gupta and Baker 2015 A. Gupta, and J. Baker, A Bayesian change point model to detect changes in event occurrence rates, with application to induced seismicity, *12th international Conference on Applications of Statistics and Probability in Civil Engineering ICASP12*, Vancouver, Canada, July 12-15, 2015.
- Niemeijer 2007 A. R. Niemeijer, C. J. Spiers, A microphysical model for strong velocity weakening in phyllosilicate-bearing fault gouges, *Journal of Geophys. Res., Solid Earth*, 112, 2007.
- KNMI 2012 B. Dost, F. Goutbeek, T. van Eck, D. Kraaijpoel. Monitoring induced seismicity in the North of the Netherlands: status report 2010.
- Pijpers 2015 F. P. Pijpers, Phase 1 update May 2015: significance of trend changes in tremor rates in Groningen. CBS report May 2015.
- Reasenbergh 1985 Reasenbergh, P. (1985), Second-order moment of central California seismicity, 1969-82, *J. Geophys. Res.*, 90, 5479-5495.
- Schcherbakov 2004 R. Schcherbakov, D.L. Turcotte, J.B. Rundle, A generalized Omori's law for aftershock decay, *Geophys. Res. Lett.*, doi: 10.1029/2004GL019808, 2004
- TNO 2013 Toetsing van de bodemdalingsprognoses en seismische hazard ten gevolge van gaswinning van het Groningen veld. TNO report 2013 R11953, 23 December 2013.
- TNO 2014a Technisch rapport behorende bij "Effecten verschillende productiescenario's op de verdeling van de compactie in

	het Groningen veld in de periode 2014 t/m 2016". TNO report 2014 R10426, 7 March 2014.
TNO 2014b	Recent developments of the Groningen field in 2014 and, specifically, the southwest periphery of the field. TNO report 2014 R 11703, 9 December 2014.
TNO 2015a	Recent developments on the seismicity of the Groningen field in 2015. TNO report 2015 R10755, 29 May 2015.
TNO 2015b	Accompanying letter with the TNO report R10755, date 22 June 2015, AGE 15-10.036.
Verberne 2014	Verberne, Berend A., Plümper, Oliver, de Winter, D.A. Matthijs & Spiers, Christopher J., Superplastic nanofibrous slip zones control seismogenic fault friction. <i>Science</i> , 346 (6215), (pp. 1342-1344), 2014.

7 Signature

Utrecht, 15th October 2015

TNO

A handwritten signature in blue ink, consisting of several overlapping loops and a long horizontal stroke extending to the right.

Dr. I.C. Kroon

Head of department

Karin van Thienen-Visser, Danijela Sijacic,
Manuel Nepveu, Jan-Diederik van Wees, Jenny
Hettelaar

Author

A Normalization of cross-correlations

The cross-correlation of two functions f and g on the real t -axis is defined as the Riemann-Stieltjes integral

$$h(k) = \int f(t)g(t+k) d\alpha(t)$$

Either we choose $\alpha = t$ or take a step function for α . In this way we incorporate (Riemann) integrals and series into one formalism (Rudin, 1976, Chapter 6). We leave the integration boundaries unspecified as yet.

Now form $Q \equiv \int [f(t) - \lambda g(t+k)]^2 d\alpha(t)$, λ being a real number. Then Q is obviously non-negative

$$\text{Hence } \lambda^2 \int g(t+k)^2 d\alpha(t) - 2\lambda \int f(t)g(t+k) d\alpha(t) + \int f(t)^2 d\alpha(t) \geq 0.$$

In order that this quadratic equation in λ satisfies this inequality for all functions f and g the discriminant should be non-positive. This leads to the general requirement that

$$\left| \int f(t)g(t+k) d\alpha(t) \right|^2 \leq \int f(t)^2 d\alpha(t) * \int g(t+k)^2 d\alpha(t)$$

If we now set the integration boundaries to $-\infty$ and $+\infty$ we retrieve the familiar Cauchy-Schwarz inequality, since k can then be omitted from the last integral for the given choices of α . We can now normalize the cross-correlation with the square root of the auto-correlations of f and g taken at lag 0, with the neat result that the cross-correlation so normalized is confined to $[-1, 1]$.

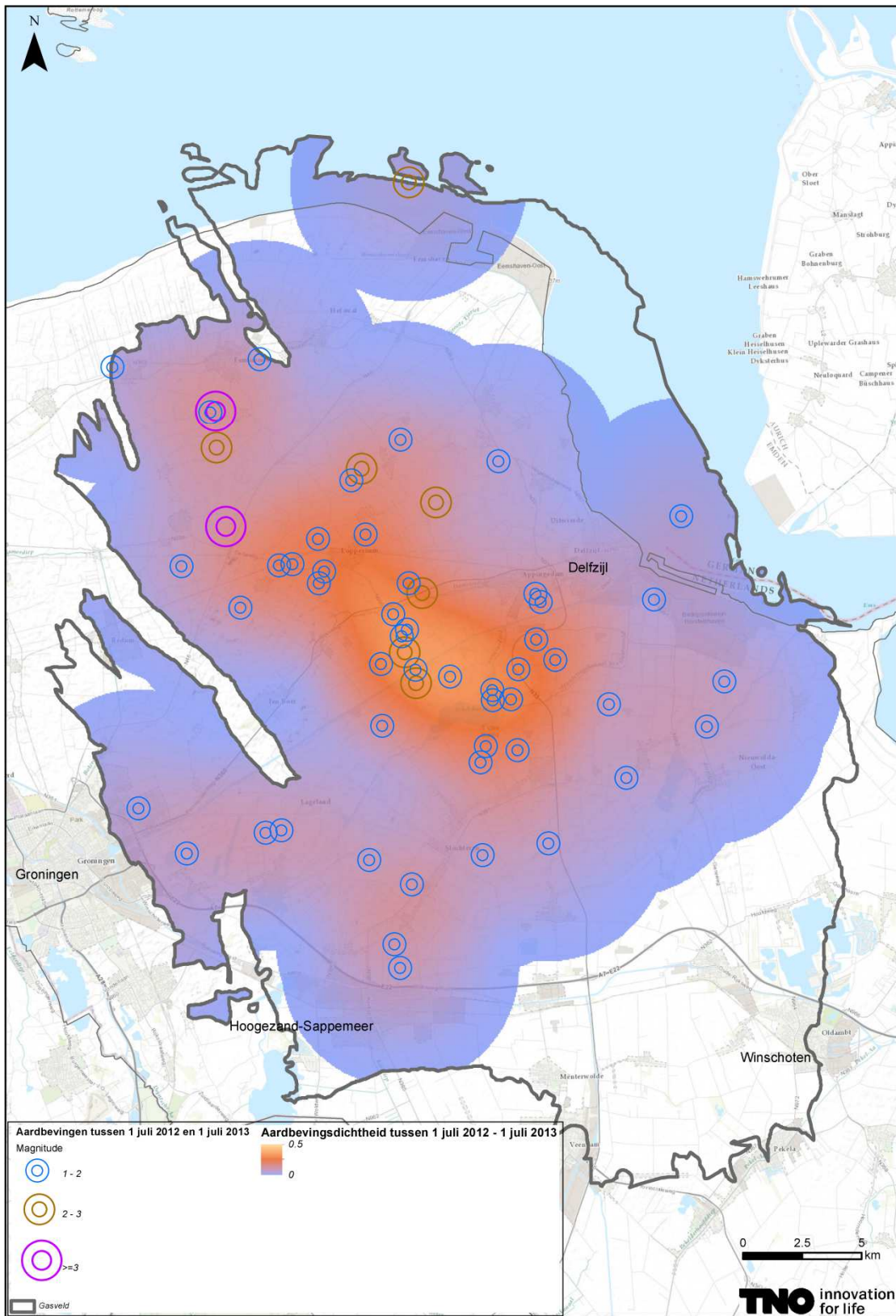
However, we are obviously dealing with data over a *finite* time interval. We normalized the cross-correlation function with the square root of the right hand side, taking $k=0$, since lag-dependent normalization gives obviously rise to distortion, which is unacceptable. But then, alas, we have no guarantee that the cross-correlation so normalized always remains between -1 and 1.

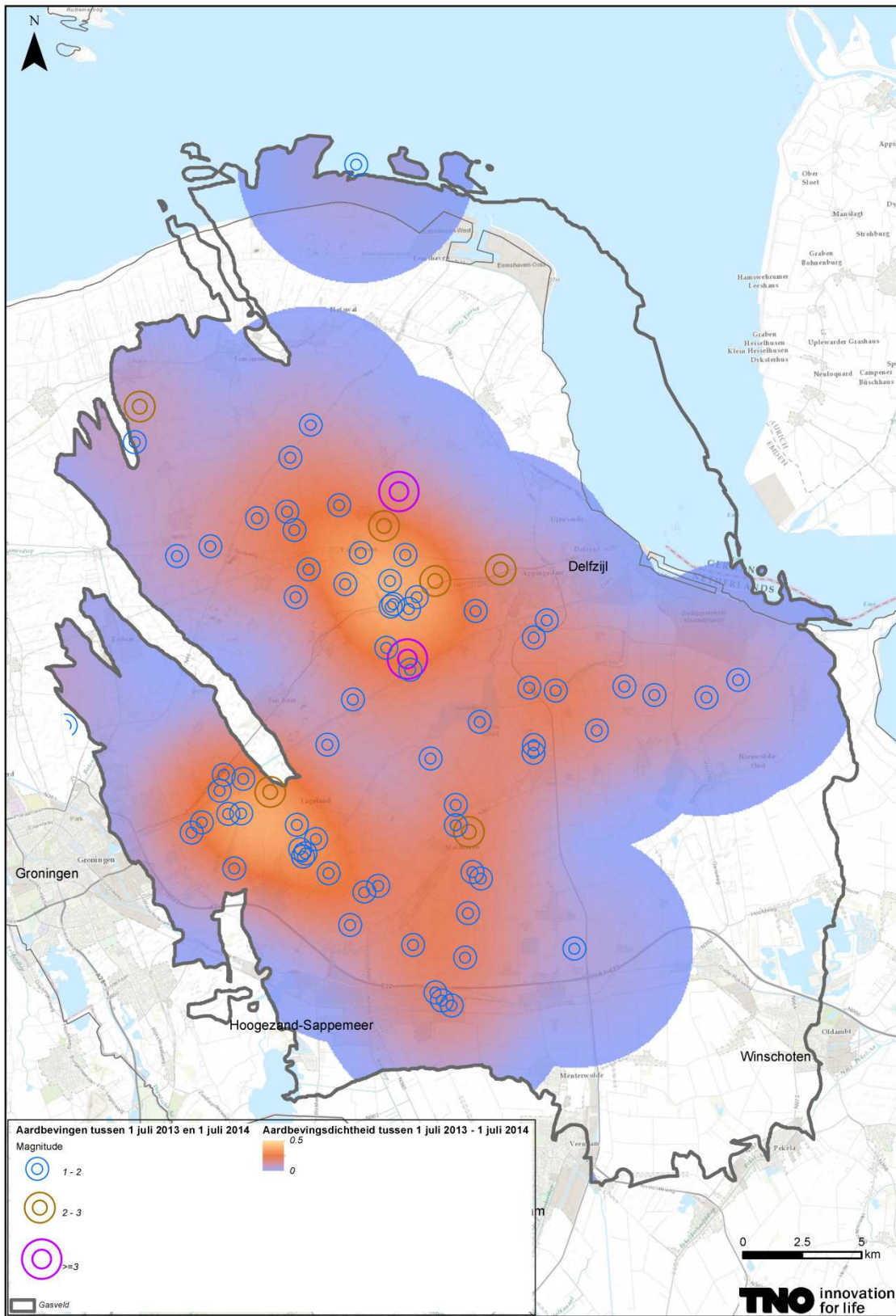
Reference

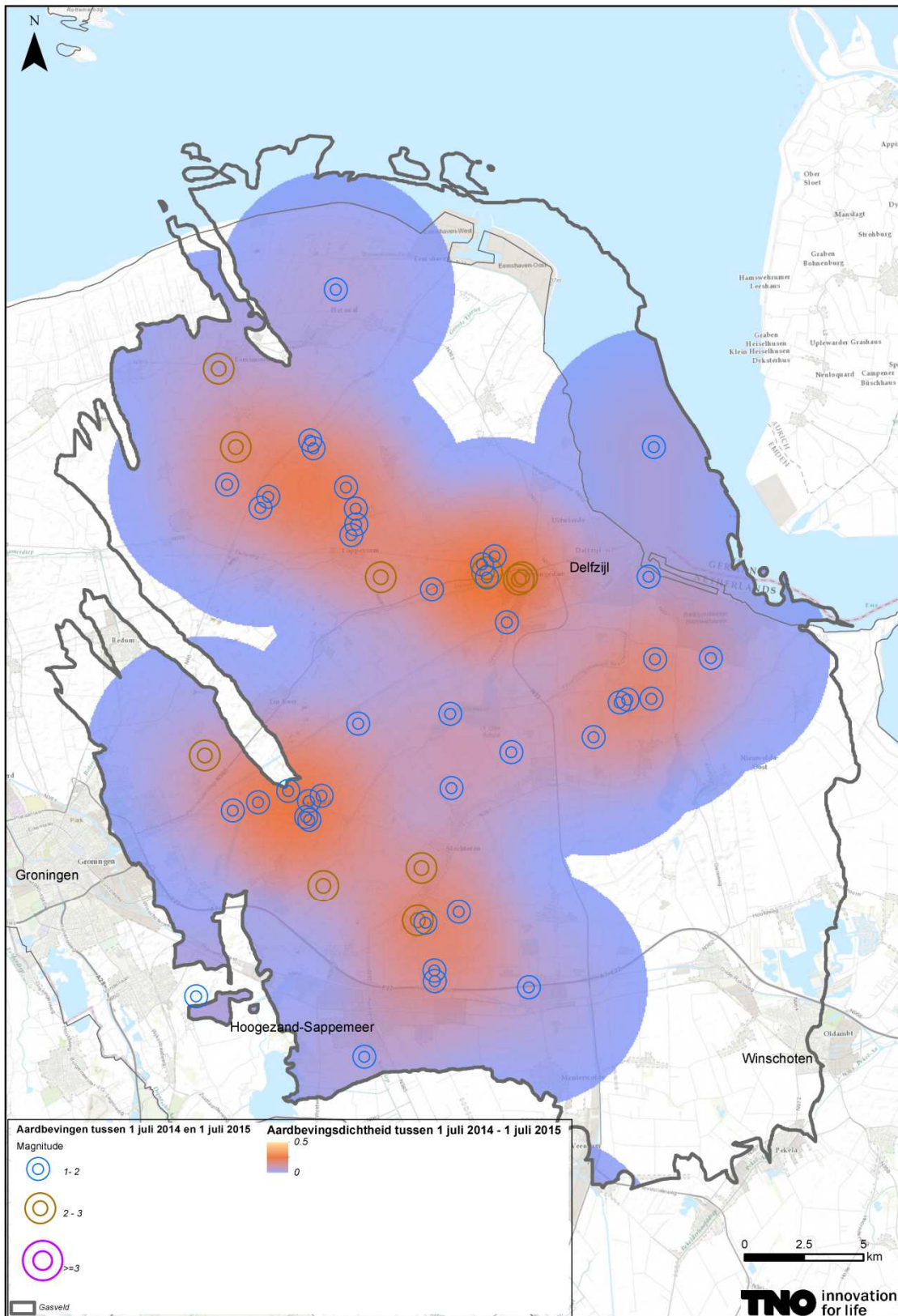
Walter Rudin, Principles of Mathematical Analysis, McGraw-Hill Kogakusha, Ltd. 1976.

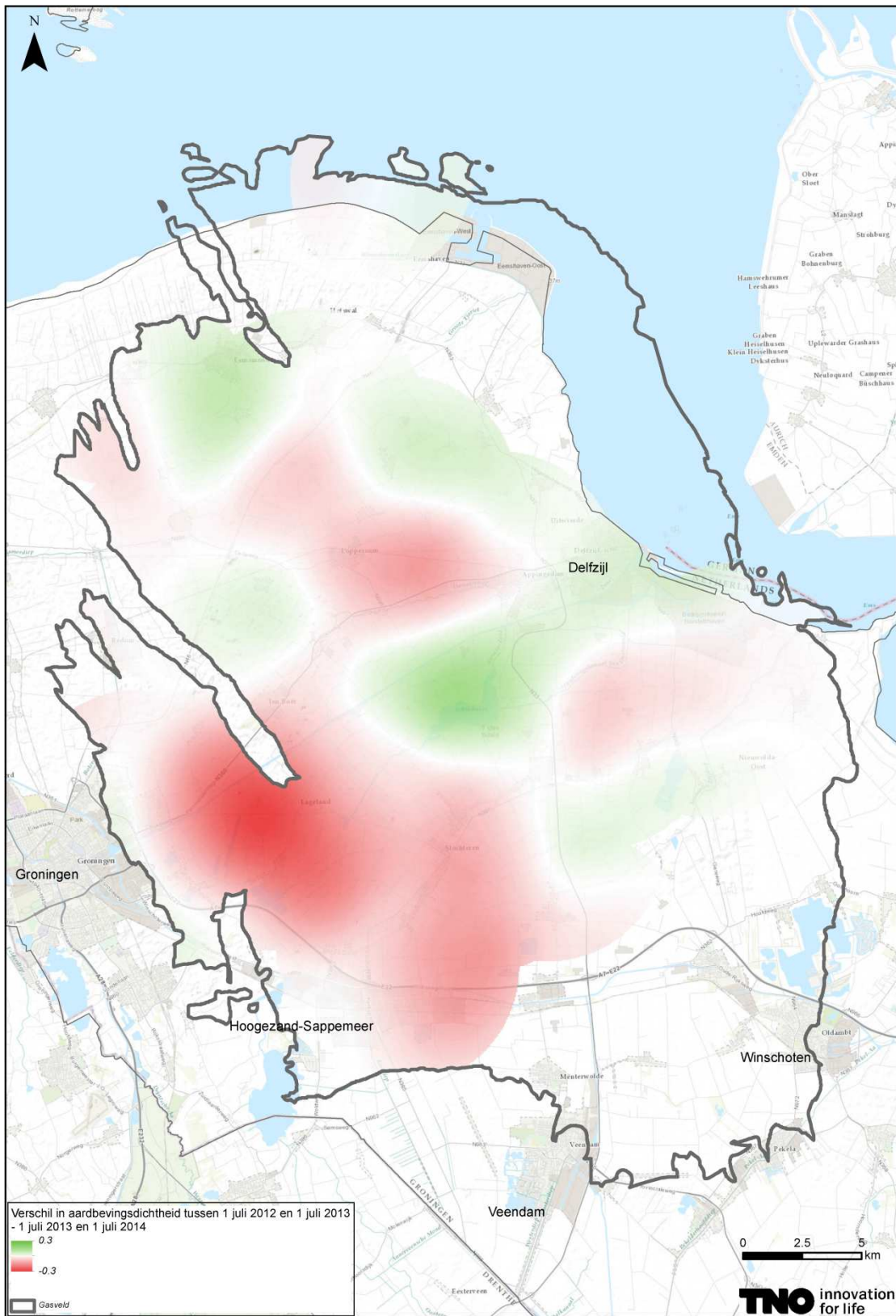
B Event density maps

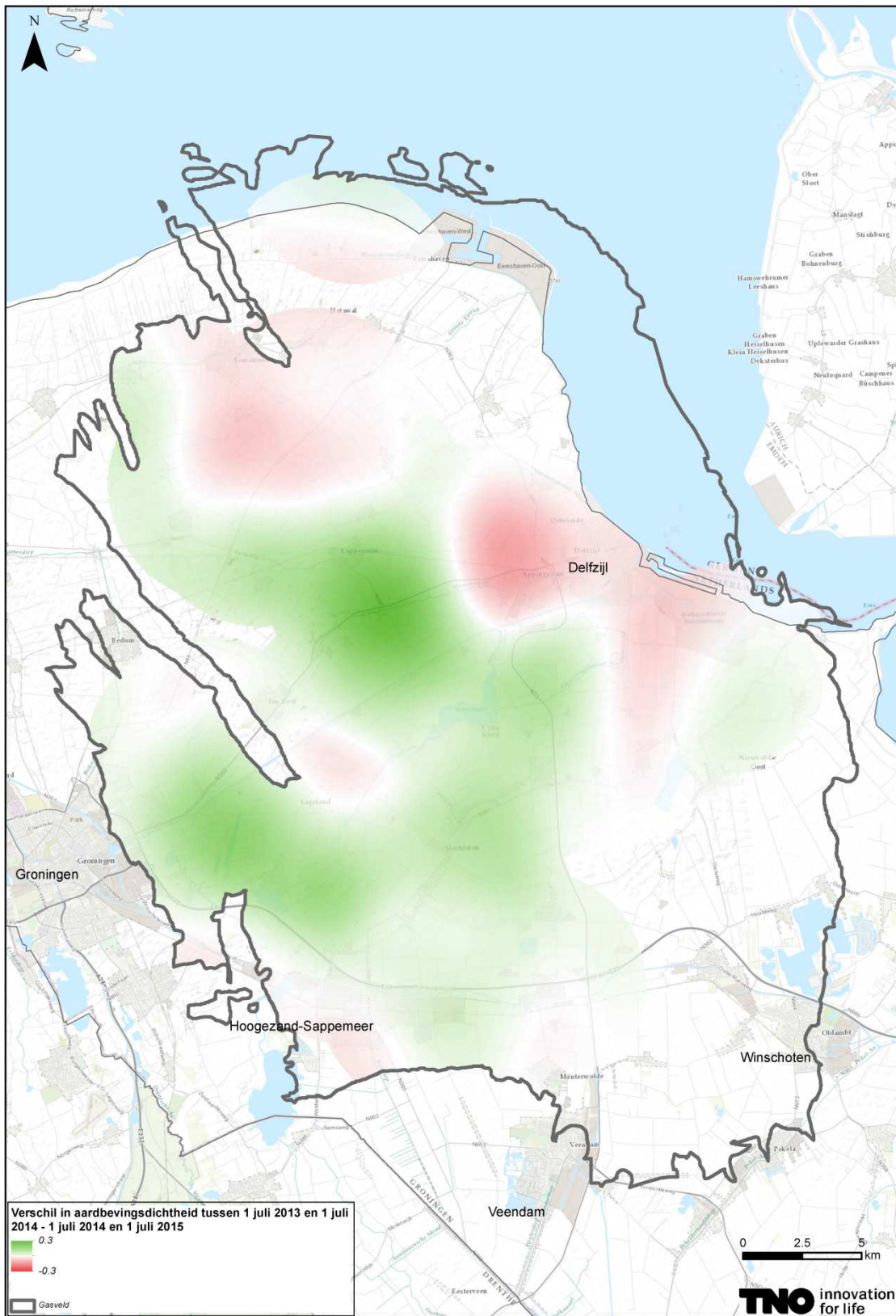
In this appendix Figure 2-8 is shown in a larger format. The figures are repeated from left to right and top to bottom and follow on the next pages.











C Production density maps

In this appendix Figure 2-2 is shown in a larger format. The figures are repeated from left to right and top to bottom and follow on the next pages.

